CHEMICAL ENGINEERING SCIENCE
GENIE CHIMIQUE

VOL. 2 JUNE 1953 NO. 3

Temperature and humidity measurements in a drying fluidized bed.

P. M. HEERTJES, H. G. J. DE BOER and A. H. DE HAAS VAN DORSSER

The Technical University, Delft, General Department of the Organisation of Applied Scientific Research, The Hague

(*Received* 20 *February* 1953)

Summary—Temperature and humidity measurements of air in and above a drying fluidized mass of silica gel are given. It is proved that perpendicular to the flow of air the temperature and the humidity show no gradient ; that the temperature of the silica gel is practically equal to the temperature of the leaving air, being independent of the place in the apparatus ; that mass and heat transfer takes place in a very small layer only and finally that heat is transferred to the solid substance by the supporting sieves as well as by the air directly.

Résumé—Les auteurs ont effectué des mesures de la température et de l'humidité de l'air dans et au-dessus d'une masse de silicagel séchéante et fluidifiée. Ils prouvent que, dans un sens perpendiculaire au courant d'air, la température et l'humidité ne présentent pas de gradient ; que la température du silicagel est pratiquement égale à la température de l'air sortant puisque cette température est indépendante de l'endroit dans l'appareil ; que la transmission de la substance et de la chaleur ne s'effectue que dans une couche très mince et enfin que la chaleur est transmise à la substance solide tant par les cribles supportants que directement par l'air.

INTRODUCTION

In the course of our studies on the drying of a fluidized mass with the aid of air it proved to be of importance to measure the temperature and the humidity of the air in the fluidized mass, as well as the surface temperature of the solid substance. As far as we could see neither the measurements of KETTENRING *et al.* [1] nor those of LEVA *et al.* [2] gave the correct air conditions in the bed. We therefore tried a different technique in obtaining the desired data. The results of our experiments will be given below.

METHOD OF INVESTIGATION

A closely graded quantity of silica gel is fluidized by means of a current of air of known quantity, temperature and humidity in a cylindrical container, – with one or more sieveplates – insulated against heat flow by means of a jacket. To measure the conditions of the air in the silica gel a tube of rather small diameter, adjustable in a horizontal and vertical direction, was inserted into the fluidized mass. Through this tube air could be sucked by means of a waterjet pump

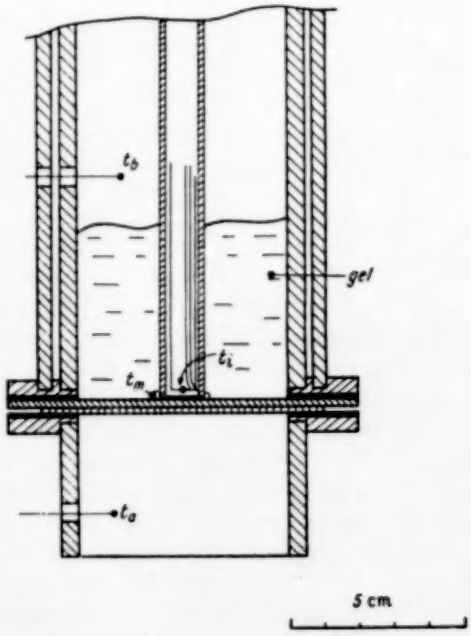

Fig. 1. Sketch of the container of the fluidization apparatus.

at an adjustable velocity. The tube could be sealed by means of sieves of different materials to prevent the silica gel entering the small tube. The following measurements were made : the temperature and the humidity of the incoming air and of the air leaving the fluidized mass ; the temperature and humidity of the air in the inner tube (on a short distance above the sealing sieve) and the temperature in the fluidized mass, measured in the same plane – perpendicular to the direction of flow – as the temperature in the inner tube.

t_b = temp. of air leaving the fluidized mass measured some cm above the surface of this mass.

t_m = temp. in the fluidized mass.

t_i = temp. of the air in the inner tube measured just above the small sealing sieve.

The humidity was measured with a Foxboro dewcell recording meter and expressed as the dewpoint.

The humidity of the incoming air was always kept constant (dewpoint in different runs ranging from 10 to 13°F ($\pm$ 0·2°F)) by passing

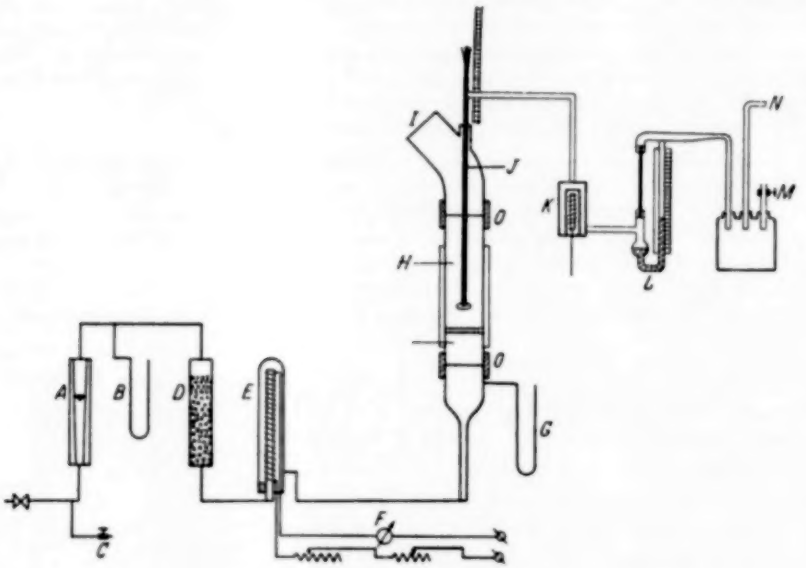

Fig. 2. Sketch of the apparatus.

A sketch of the fluidization apparatus used, drawn as far as possible to scale, is given in Fig. 1. The cylindrical vessel and jacket were made of *Plexiglass*, the inner tube of glass. The main sieve used was of celluloid. Temperatures were measured with thermocouples of copper-constantan with a small welded point and as great a length of wire as possible in an equithermal plane, via the compensation method. An exception was made for the incoming air, the temperature of which was measured with a small mercury thermometer. The temperatures measured were :

t_a = temp. incoming air, measured some cm below the sieves.

dry air (tapped from the compressed air system, after the removal of liquid water) through a bed of blue silica gel. The temperature of this air could be adjusted by means of an electrically heated wire with adjustable current. The quantity of air was measured with a flowrator.

The humidity of the air sucked through the inner tube and of the leaving air were again measured with the Foxboro meter the quantity of the air passing the inner tube measured by means of a capillary tube flow meter, later with a flowrator.

A sketch of the whole set-up is given in Fig. 2. *A* is the flowrator for the incoming

VOL. 2 1953

air, *B* and *G* open manometers, *C* and *M* are regulators to adjust the quantity of air, *D* contains the blue silica gel, *E* is the heater with wire, resistances and ammeter *F*, *H* is the jacketed fluidization apparatus of a somewhat different kind as given in Fig. 1. (no changeable sieves). *J* is the inner tube ; at *I* a tube could be attached to measure the humidity. *K* contains the dewcell of the humidity meter ; *L* is a flow-meter ; *O* are two india-rubber tubes and finally at *N* the vacuum pump was connected. *E* and *H* were insulated by means of cottonpads.

As variables in the measurements were chosen, time, the places of measurements in and above the fluidized silica gel, the flow rate and temperature of the incoming air, type and number of sieves used to support the silica gel and of the small sealing sieve(s) for the inner tube.

Silica gel of about one size, namely 0·3-0·5 mm, was used with a constant initial water content of 42·8% of water calculated on the dry substance. Reproducible initial amounts of water in the gel could be easily obtained by fluidizing the gel in a separate apparatus with moist air, humidified in two packed towers filled with Raschig rings and water. After the towers, the air passed a separator to catch the entrainment. The whole set was placed in a thermostat at 20°C. A sharp indication for the endpoint of the humification was a constant temperature in the gel.

The Results Obtained

(a). *The entrance effect* (e)

A typical set of curves of a normal run is given in Fig. 3 where t_b and t_a are given as a function of the drying time. The temperature of the leaving air initially falls off very rapidly and then increases again rather rapidly, becomes constant during a certain period (which will be called the constant rate period of drying throughout this paper) and finally rises again reaching assymtotically the temperature of the incoming air. In Fig. 3 is also included the temperature in the inner tube placed in the centre of the vessel (as in most measurements) without the sealing sieve, directly on the apparatus sieves ; t_i at 0 mm above the sieves ($= t_{i0}$). The amount of air sucked through the inner tube was equal to $\frac{(d_u)^2}{(D_i)^2} \times$ total amount of air, d_u being the outside dia meter of the inner tube, D_i the inside diameter of the apparatus.

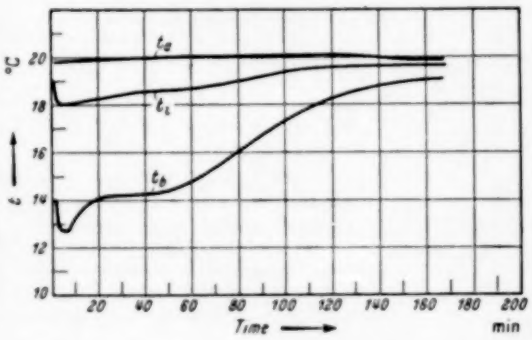

Fig. 3. t_a, t_i and t_b as a function of the time of drying.

It is clear from Fig. 3 that $t_{io} < t_a$. From this it can be concluded that the heat transfered from the incoming air to the fluidized substance is transported in at least two ways viz. (*a*) directly and (*b*) via the supporting sieves by contact between substance and sieves (see also the measurements of Leva *et al.* [2]). In our case even with an adiabatic apparatus there will be a heat exchange as well with the walls of the apparatus, changing in sign during the operation.

Neglecting these and other heat exchanges the ratio $e = \frac{t_a - t_{io}}{t_a - t_b}$ is a measure for the transfer of heat to the gel by means of the supporting sieves. We found that, within the accuracy of our determinations (0·1°C) and excluding the first 5 minutes of every experiment for obvious reasons, e is independent of the time of drying. As an example in Table I the results for three experiments differing in quantity of air are given.

It is clear that e besides being a function of the air velocity as shown in Table 1, also must depend on the material of which the sieves are made, the thickness of the sieves and the

Table 1. *e as a function of the time of drying.*

	time (min) →	5	10	20	30	40	50	60	70	80
e	Flux 36·4 l/min	0·42	0·47	0·45	0·45	0·43	0·43	0·43	0·45	0·46
	Flux 64·2 l/min				0·28	0·29	0·26	0·25	0·25	0·26
	Flux 84·1 l/min			0·20	0·21	0·22	0·20	0·19	0·18	0·14

	time (min) →	90	100	110	120	130	140	150	160	170
e	Flux 36·4 l/min	0·43	0·42	0·44	0·43	0·42	0·41	0·42	0·42	0·40
	Flux 64·2 l/min	0·25	0·29	0·27	0·24	0·28	0·27			
	Flux 84·1 l/min	0·27								

The temperature of the incoming air in all cases was about 20°C, the initial amount of wet silica gel 95 g. Drying was in all cases continued until a water content of about 10%.

VOL. 2 1953

free passage of the sieves. This holds good for the supporting sieves as well as for eventual sealing sieves of the inner tube. In Fig. 4 some

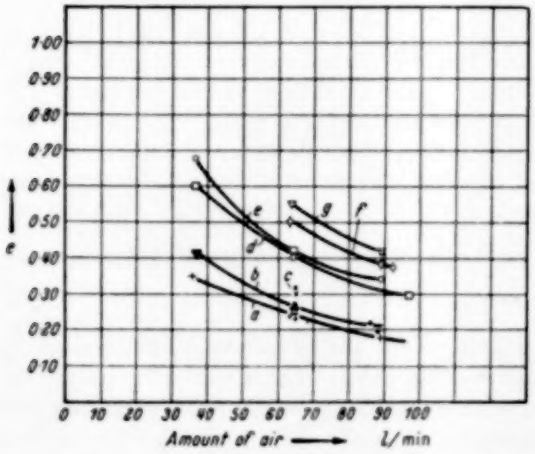

Fig. 4. The entrance effect (*e*) as a function of the amount of air and with different systems of sieves.

data obtained with experiments using differing systems of sieves have been collected. *e* was measured at the " constant rate " period, because this facilitates the measurements. In all cases the inner tube rested on the supporting sieves in the centre of the apparatus. In the direction of flow the air passed respectively :

	apparatus	*inner tube*
(a)	Nickel gauze/celluloid sieve/	—
(b)	copper sieve/celluloid sieve/nickel gauze	—
(c)	nickel gauze /celluloid sieve/	nickel gauze
(d)	celluloid sieve/copper sieve	celluloid sieve
(e)	copper sieve/celluloid sieve /copper sieve	celluloid sieve
(f)	copper sieve/celluloid sieve /nickel gauze	celluloid sieve
(g)	copper sieve/celluloid sieve /nickel gauze	celluloid sieve

The celluloid sieve of the apparatus was always the same, 2 mm thick with 33 holes of 0·4 mm diameter per cm², the small celluloid sieves applied to the inner tube differed in free passage – which was rather small – decreasing from *d* → *g*. The nickel gauzes of 0·065 mm thickness had a rather large free passage, containing 1800 holes of 70 μ diameter per cm², whereas the copper sieve was fabricated by drilling 80 holes of 0·5 mm diameter per cm² in a copper plate of 0·5 mm thickness. No further quantitative data about the sieves used

will be given here because no effort to calculate the entrance effect has been done. It can be mentioned however that under simplifying assumptions regarding the type of flow under and through the sieves, it has been possible to calculate the decrease in temperature over the sieves, assuming heat is transfered in the sieves by conduction. This calculated decrease was of the same order of magnitude as found.

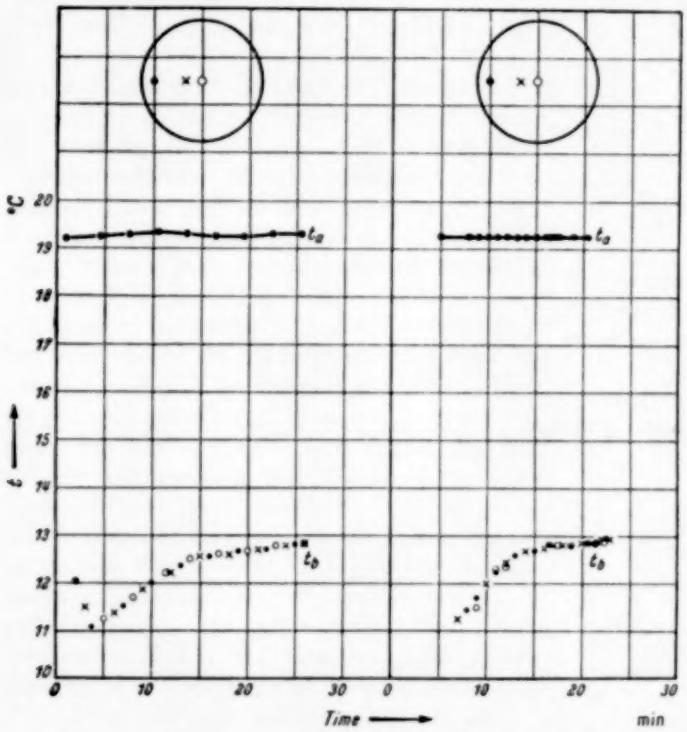

Fig. 5. The temperature of the air above the gel measured at different places in a horizontal plane.

The data collected in Fig. 4 prove that indeed e depends on air velocity as well as on the material, thickness and free passage of the sieves. The entrance effect will be small with very thin sieves with a large free passage and of a material of low conductivity. Also the higher the air velocity, the smaller will be the entrance effect. Within the range of velocities used $e \propto (\text{velocity})^{-0.7}$.

The entrance effect strongly hinders the study of heat and mass transfer problems in fluidized systems, which otherwise looks rather inviting in view of the homogenity as far as the dimensions of the apparatus is concerned.

(b) *Temperature and humidity measurements in planes perpendicular to the direction of flow.* It seemed interesting to know whether there would be a temperature or a humidity gradient in planes perpendicular to the direction of flow i.e. in horizontal planes.

Above the fluidized mass the temperature as well as the humidity of the air shows no gradient in a horizontal plane as far as the possibilities of measurement could show, as can be seen from the Figs. 5 and 6. In Fig. 5 two experiments are given, I with 95 g of wet gel and the temperature measured 2 cm above the fluidized mass at three places as indicated; II with 50 g of wet gel, measured at three places 4 cm above the mass. In both cases the temperatures plotted against time, show that there exist no differences between the three places.

In Fig. 6 the dewpoints measured in the centre of the apparatus (0) and 6 mm from the wall (x) as well as the temperature t_a are plotted against time and again show that there is no gradient. In this last case 95 g of wet gel was used, the plane was 2 cm above the fluidized mass. In all the three experiments about 65 litres of air passed through per minute.

In accordance with the above results the air in the gel also showed no appreciable gradient in a horizontal plane.

In Table 2 some of the results obtained are given. As a measure for the air temperature is given e_{ix} expressed in % based on t_i a distance x mm from the supporting sieves. At the same time t_m (the temperature in the fluidized mass) was measured and arbitrarily will be represented in the number e_{mx} in %, based on $e_{mx} = \dfrac{t_a - t_{mx}}{t_a - t_b}$

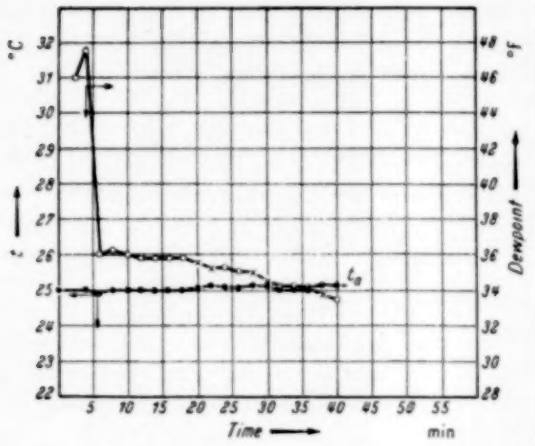

Fig. 6. The dewpoint of the air above the gel measured at different places in a horizontal plane.

100%, in which t_{mx} is the temperature in the mass at a distance of x mm from the supporting sieve. All numbers were based on measurements during the constant rate period. e_{ix} and e_{mx} are given as a function of the distance from the centre of the apparatus expressed in parts of the radius of the apparatus.

Table 2. e_{ix} and e_{mx} as a function of the distance from the centre of the container.

Distance in radii				0·2	0·54	0·67
e_{io} in %				30	32	30
Distance in radii				0·27	0·67	0·93
e_{mo} in %				75	88	82
Distance in radii	0	0	0	0·1	0·47	0·67
$e_{i1\frac{1}{2}}$ in %	48	47	45	47	48	47
Distance in radii	0·35	0·35	0·54	0·60	0·80	0·93
$e_{m1\frac{1}{2}}$ in %	77	82	77	75	88	95

of the container.

All experiments were carried out at the same velocity of 64 l/min, 95 g of wet gel was used, the temperature $t_a = 20,5$°C, the apparatus had a nickel gauze under the celluloid sieve, the inner tube was sealed with a nickel gauze.

In two other experiments using 95 g and 50 g of wet silica gel, using the nickel gauze/celluloid sieve and the inner tube resting on the celluloid sieve, at the distances of 0 and 0·54 radii from the centre was found : e_{io} resp. 24% and 24% ; e_{mo} : 81% and 78%. From these examples it is clear that the air temperature *in* the fluidized mass is also constant in a horizontal plane. The temperature t_m, as is evident, is lower than the air temperature in the gel, moreover it is not constant. It can be concluded therefore that this temperature (as has been done by others) cannot be taken for the temperature of the air in the gel, because it represents a mean temperature of air and surface temperature of the gel ; moreover the surface temperature of the silica gel must be lower than the air temperature and finally this mean temperature will depend on the frequency of contact of the thermo-couple with the gel. There is a tendency that the mean temperature at the wall is lower than in the midst of the apparatus. This would mean a higher concentration of gel at the wall, which again would tally with the observed movements in the fluidized bed, the particles going up in the centre and coming down near the wall. The values of t_m however are not very reliable, and as the authors see it, ought not to be used.

It should be remarked here that the authors have found a definite difference in pressure between the air in the midst of the apparatus and at the wall, measured in a horizontal plane 1 cm above the sieve, the air in the midst showing a *smaller* pressure. Differences in pressure-difference with the air outside the apparatus up to 8% could be found.

It can be concluded from this paragraph that within the accuracy of the determinations the air in the apparatus in and outside the fluidized mass shows no temperature, nor a humidity gradient in a horizontal plane. The air quite near the wall was not included in the observations, therefore also not in the conclusion.

VOL. 2 1953

(c) *The temperature of the fluidized gel.*
As has been said in paragraph (b) the mean temperature in the fluidized mass is lower than the air temperature t_i in the gel and therefore the surface temperature of the silica gel must be lower than this temperature t_i.

In the next paragraph (d) it will be discussed why the authors are of the opinion that the temperature t_i, measured in all cases while a quantity of air is sucked through the inner tube equal to $\frac{(d_u)^2}{(D_i)^2} \times$ the total quantity of air gives a fair approximation to the air temperature, if a thin nickel-gauze of large free passage is used as a sealing sieve. (d_u = outside diameter of the inner tube, D_i = inside diameter of the container).

In this paragraph it will be discussed how the authors have tried to evaluate the surface temperature of the fluidized mass.

During a normal drying experiment the inner tube was removed. A thermocouple which could be replaced in a vertical direction was placed in the axis of the apparatus. The temperature t_b was measured above the fluidized mass as a function of the time. At intervals the thermocouple was moved into the bed to a height of about 2 cm above the sieves, the air supply stopped and after about 10 seconds the temperature read. Prolonging the time to about one minute did not change this temperature in a measurable way.

Then the couple was moved upward, the air supply opened again and the measurements repeated. Two typical temperature-time curves are given in Fig. 7. The temperature t_b (above the bed) is given as points (·), the temperature in the bed by points (0). These points indicate that the temperature of the gel is almost equal to the air temperature above the bed, with a possible difference of the accuracy of the temperature measurements, viz. 0·1°C. The small amount of stagnant air present has practically no influence on the temperature.

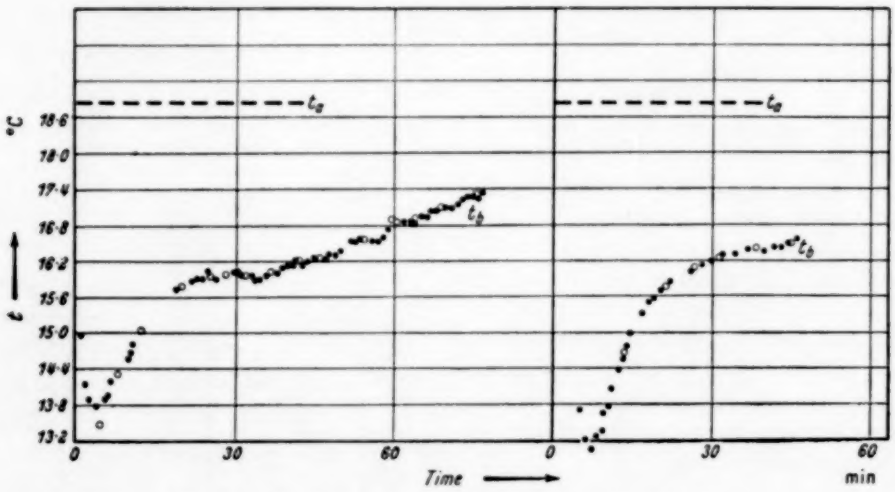

Fig. 7. The temperature of the gel (0) compared with the temperature t_b of the air above the gel (.).

Near the supporting sieves the procedure described above could not be followed, because the hotter sieves transported heat to the thermocouple too quickly, hindering the measurements. By following the behaviour of a thermocouple inserted into the fluidized mass indicating t_m at a height of 1½ mm above the sieves,

it was however observed that after closing the air supply the temperature of t_m fell rapidly and then rose rapidly again. The lowest temperature observed was only some tenth of a degree centigrade higher than t_b above the gel.

Because of the very small particles used, causing an equalising time of the temperatures in the gel to differences $<$ than 0·1°C of some tenth of a second if initially these temperature differences are of the order of 10°C, as can be calculated with the aid of the Fourier number, it will be clear that the temperature of the gel measured is a mean mass temperature and not a surface temperature.

On the other hand for the same reason the temperature differences in the gel will be small, and with these small particles therefore a distinction between surface temperature and mean mass temperature has no real practical meaning. Therefore the temperature measured is called the temperature of the gel.

From the observations the conclusion seems warranted that under the conditions used in our experiments, after a short time of drying the temperature of the fluidized gel at any time is almost equal to the temperature of the air leaving the bed and independent of the place in the bed.

The actual temperature drop existing between the sieves and the gel in contact with the sieves could not be measured.

(d) *The temperature and the humidity of the air in the fluidized bed in a vertical direction*

By moving the inner tube in a vertical direction the temperature and the humidity of the air in the fluidized mass at different heights could be measured. The measurements were all carried out with the tube in the axis of the apparatus and to facilitate the measurements during the constant rate period of drying.

As said before it still has to be proved that the air in the tube in reality gives the air conditions in the fluidized mass as wanted. To prevent the removal of solid substances the inner tube had to be sealed with a sieve. For this we chose a very thin nickel gauze of large free passage (see section (a), p. 99).

To prove that the temperature and humidity measured closely approximate the desired values the following sets of experiments were carried out.

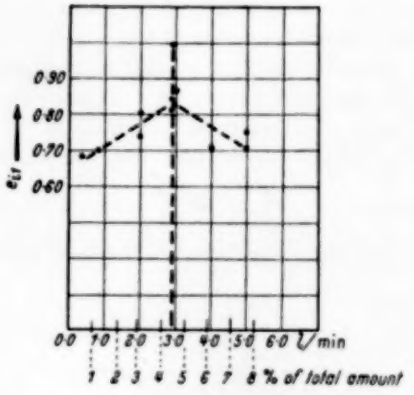

Fig. 8. ϵ_{i1} of the air sucked through the inner tube, (placed 1 mm above the copper sieve) as a function of the amount of air.

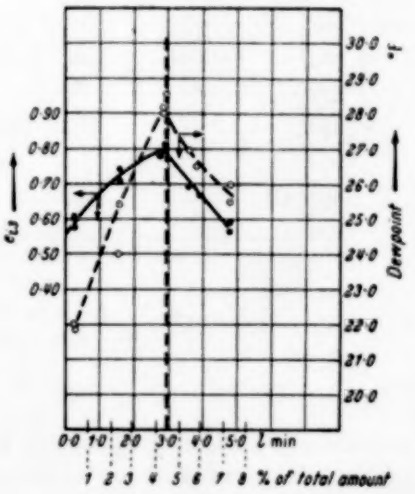

Fig. 9. ϵ_{i3} and the dewpoint of the air sucked through the inner tube (placed 3 mm above the celluloid sieve) as a function of the amount of air.

In the first set the humidity and t_i were measured with different amounts of air sucked through the inner tube. The results obtained are collected in Figs. 8 and 9 in which $\epsilon = \dfrac{t_a - t_i}{t_a - t_b}$ and the

dewpoint are given as a function of the amount of air passing the inner tube, expressed in litres per minute and in % of the total amount. Measurements were again carried out at the constant rate period. The tube was 1 mm (Fig. 8) and 3 mm (Fig. 9) respectively above the sieves.

Both the curves obtained show a maximum. The amount of air passing the inner tube normally used in our experiments was as stated $\frac{(d_u)^2}{(D_i)^2} \times 100\%$. As $d_u = 1{\cdot}26$ cm and $D_i = 6{\cdot}0$ cm, this amounts to 4·4%. Both maxima lie approximately at this velocity (see dotted vertical lines)

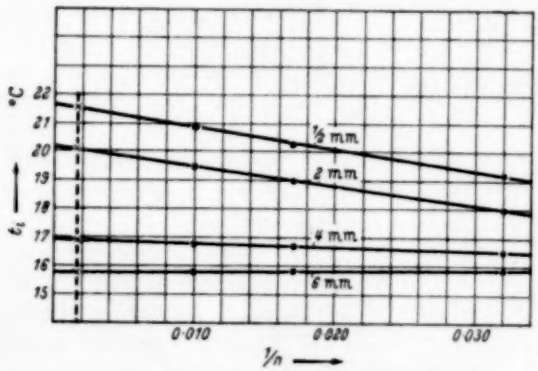

Fig. 10. t_i as a function of the reciprocal number of holes (1/n) in the scaling sieve, measured at different heights.

At velocities higher than 4·4% part of the substance is sucked against the nickel gauze causing less movement of this part, resulting in an accelerated drying giving relatively higher temperatures and lower humidities. At lower velocities than 4·4% the air will have had a less intensive contact with the fluidized mass resulting again in relatively higher temperatures and lower humidities.

In the second set of experiments the influence of the nickel sieve on t_i was measured. As has been shown this sieve can have influence on the temperature, by the solid substance moving along its surface and taking up heat, decreasing the temperature of the sieve and therefore of the air that has passed through it.

A set of experiments was now carried out, using sieves of celluloid of the same thickness (0·25 mm) and with an increasing number of holes of the same diameter (0·2 mm). The temperature t_i obtained under the same conditions, at an amount of 4·4% from the total of air passing the inner tube, and measured at the constant rate period, is plotted in Fig. 10 against the reciprocal number 1/n of the holes. The values of t_i extrapolated from this figure to the maximum of holes possible, calculated from the total area of the tube (see dotted vertical line), are given in Table 3 for four different distances from the supporting sieve. In the same table t_i as measured with the normal nickel gauze as a sieve and for the same conditions are given.

From these data it can be concluded, that the nickel gauze used does not decrease the temperature of the air if the tube is placed in the gel.

It must be remarked however that if the distance of the inner tube to the supporting sieve = 0 mm, so that the nickel gauze is in contact with this sieve, a decrease in the temperature t_i is observed, which amounts to about 0·3°C under the conditions described.

From these two sets of experiments it is clear that t_i as measured in fair approximation gives the temperature of the air as desired.

It may be remarked here, that inevitable disturbances in the bed caused by the insertion of the inner tube, seem to be of no great influence, if the distance of the tube to the supporting sieves is not too small.

Table 3. *Determination of t_i for different sieves.*

Distance from supporting sieve in mm	½	2	4	6
t_i extr. for total free tube in °C	21·6	20·1	16·9	15·8
t_i determined with nickel sieve in °C	21·3	20·3	17·0	15·8

The results of measurements of the temperature and the humidity of the air in a vertical

direction in the fluidized mass for the case in which the amount of air was 65 l/min, the amount of wet silica gel was 95 g and the celluloid sieve was used, are represented in Fig. 11, in which t_i, t_m and t_b and the dewpoint are plotted against the distance from the sieve in mm. The inner tube was in all cases sealed with a nickel gauze. The total height of fluidized mass was about 60 mm. Point A in Fig. 11 gives the temperature t_i if the inner tube is not sealed with a nickel gauze (see above). In Fig. 11 also the temperature t_a and the dewpoint of the incoming air, as well as the dewpoint of the leaving air are given.

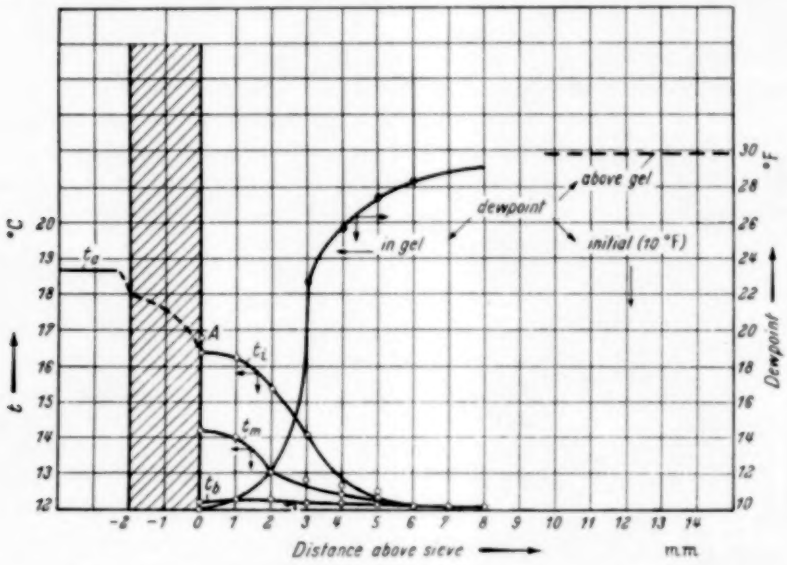

Fig. 11. The temperature and the humidity of the air as a function of the distance above the supporting celluloid sieve.

In Fig. 12 the temperature measurements obtained with the copper sieve mentioned before, instead of the celluloid sieve are represented. The conditions are the same as regards quantity of air and amount of substance. The temperature given in Fig. 12 is a temperature measured with a thermocouple pressed under and against the sieve. A same result was obtained in the experiments collected in Fig. 11 (not given).

The conclusion of these experiments is that heat exchange and mass transport take place practically only in the first 4-6 mm of the bed, whereas the rest of the bed is inactive in this respect. For drying apparatus this is important as far as the height of the drying bed and therefore the construction of the apparatus is concerned.

That the dewpoint after 6 mm has not yet fully reached the maximum value may be due either to some lag in the measuring device, and, or to the diffusion of water vapour from the pores of the solid substance to the main stream of air.

The differences in the form of the t_i — distance lines in both cases may be caused by the difference in sieves used, causing a different movement of the particles over the sieve surface.

The conclusion given is supported by experiments done with different amounts of substance,

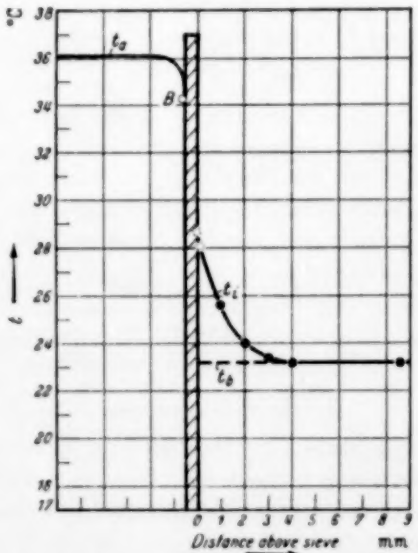

Fig. 12. The temperature of the air as a function of the distance above the supporting copper sieve.

VOL. 2 1953

dried under the same conditions (amount and temperature of air, and sieves used). The results are collected in Fig. 13 giving the temperature t_b (×), the temperature t_m (+) and t_i (·) measured 0 mm above the sieve, and the dewpoint (0) of the leaving air as a function of the amount of gel, all measured during the constant rate period. Because the measurements at low quantities of substance are extremely difficult and not very reliable, due to the short period of constant drying conditions, relatively bigger influences of the walls (causing an increase in t_b while t_i is constant) and poor fluidization (see t_m), Fig. 13 warrants the conclusion that heat transfer takes place for the greater part only at the surface of and in a rather thin layer above the supporting sieves. This layer was in our experiments about 5 mm thick.

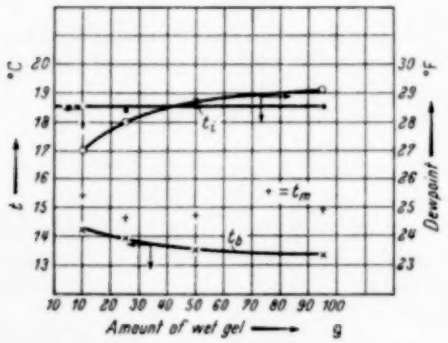

Fig. 13. t_i, t_b, t_m and the dewpoint of the air as a function of the amount of gel.

As far as heat transfer alone is concerned, it can be calculated from data given in the literature that under the conditions mentioned, the heat exchanging layer is about 2-3 mm thick if a difference of 0·1°C is assumed between leaving air temperature and surface temperature.

Conclusions

Within the limitations given by the conditions used the following conclusions can be given for the drying of a fluidized bed of silica gel with air in an adiabatic apparatus using a supporting sieve and vertical flow of air :

(*a*) The air temperature and humidity are independent of the place in the apparatus in a horizontal direction ;

(*b*) The temperature of the gel is independent of the place in the apparatus and equal to the temperature of the air leaving the bed ;

(*c*) Heat is transferred to the gel in at least two ways ; by means of contact of the fluidized substance with the sieves and by means of contact with the air. The ratio of the amount of heat transferred by the sieves over the total amount transported is independent of the time of drying. The ratio decreases with increasing air velocity but increases with decreasing free passage in the sieves and with increasing thickness of the sieves.

(*d*) Practically all heat and mass transfer takes place in a rather thin layer above the sieves. The depth of this layer does not depend appreciably on the amount of substance fluidized.

Notation

ε = The entrance effect $= \dfrac{t_a - t_{io}}{t_a - t_b}$. (No dimension).

$e_{ix} = \dfrac{t_a - t_{ix}}{t_a - t_b}$ (No dimension).

$e_{mx} = \dfrac{t_a - t_{mx}}{t_a - t_b}$ (No dimension).

} A certain ratio of temperature difference measured x mm above the sieves. e.g. e_{i1}, e_{i3}.

d_u = Outside diameter of inner tube (cm).

D_i = Inside diameter of the container (cm).

t_a = Temperature of the air entering the apparatus (°C).

t_b = Temperature of the air leaving the fluidized mass (°C).

t_{mx} = Mean temperature of the fluidized mass and air, measured x mm above the sieves. (°C).

t_{ix} = Temperature of the air in the inner tube of the apparatus, measured x mm above the apparatus sieves. (°C).

References

[1] Kettenring, K. N., Mandersfield, E. L. and Smith, J. M. ; Chem. Eng. Prog. 1950 **46** 139. [2] Leva, M., Weintraub, M. and Grummer, H. ; Chem. Eng. Prog. 1949 **45** 563.

Chemical Engineering Science, 1953, Vol. 2, pp. 108 to 119. Pergamon Press Ltd.

Hydroextraction V: Radial distribution of pressure in homogeneous and banded cakes

M. M. Haruni and J. Anderson Storrow

Chemical Engineering Laboratory, Applied Chemistry Department, College of Technology, Manchester

(*Received* 7 *July* 1953)

Summary—Hydroextraction and filtration permeabilities have been measured in a 9 in. dia. perforated basket centrifuge for cakes formed from layers of kieselguhr of high, and of starch and of chalk of low permeability. Conditions that lead to discontinuity in the development of centrifugal head in the liquid within a heterogeneous cake are absent from cakes of one material. The results justify the assumption that the latter cakes run with their void space full of liquid and that atmospheric pressure is transmitted to the outer surface of the cake in a hydroextractor. This flow pattern is the fundamental basis of the proposed equations for hydroextraction.

Résumé—Dans un panier d'essoreux centrifuge de 225 mm. de diam. l'auteur détermine les perméabilités pour l'essorage et pour la filtration de couches alternées de kieselguhr (haute perméabilité) et d'amidon ou de craie (faible perméabilité). Avec des gateaux homogènes, on ne retrouve pas les conditions qui conduisent à l'établissement d'une discontinuité dans la force centrifuge agissant sur le liquide présent dans un gateau hétérogène.

Ces resultats justifient l'hypothèse qu'un tourteau homogène tourne avec ses pores remplis de liquide et que la pression atmosphérique progresse vers la surface externe dans l'essoreux. Cetter forme d écoulement est prise comme base pour les equations de l'essorage, proposées por l'auteur.

VOL. 2 1953

It has been shown elsewhere [1], [3] that the flow of a liquid through a hydroextractor cake of constant permeability K follows the relationship

$$q = \frac{4\pi^3 n^2 XK}{\mu g} \cdot \frac{(r_0^2 - r_L^2)}{\log_e r_0/r_e} \qquad (1)$$

when the centrifugal head generated in the system is resisted only by viscous shearing forces in the laminar motion of the fluid within the cake.

It has been shown [2] that the permeability of the innermost layer may be 25% greater than that of the outermost layer of a thick cake. A cloth-cake interface resistance, R, was assumed to affect both processes of hydroextraction and filtration. Thus the general form of equation (1) for a cake composed of layers becomes :

$$\frac{4\pi^3 n^2 X (r_0^2 - r_L^2)}{\mu g \cdot q} = \frac{\log_e \frac{r_0}{r_1}}{K_1} + \frac{\log_e \frac{r_1}{r_2}}{K_2} + \ldots + \frac{\log_e \frac{r_{n-1}}{r_n}}{K_n} + R \qquad (2)$$

These equations were based on the equality between the centrifugal head, P_c, and the energy dissipated in friction through the cake, P_F, assuming that the pressure is atmospheric at r_L and r_0 and that the cloth support is running "empty," i.e. without the void space in the cloth being completely filled with liquid [2].

It is of value to study the pressure distribution through a cake and the effect of a highly permeable layer in a cake, in order to assess the validity of the assumed flow mechanism.

The pressure distribution will first be considered for a case conforming to equation (1), the modifications appropriate to the system for equation (2) being considered later.

The pressure terms are defined for a uniform cake as :

$$P_c = \tfrac{1}{2} \cdot \frac{(2\pi n)^2}{g} \cdot (r_0^2 - r_L^2) \qquad (3)$$

$$P_F = \frac{1}{K} \cdot \frac{\mu q}{2\pi X} \log_e \frac{r_0}{r_e} \qquad (4)$$

At a constant speed of revolution, P_c, will be proportional to $(r_0^2 - r_L^2)$, and is zero at $r = r_L$.

Curves *A*, *B* and *C* in Fig. 1 represent the values of P_c at all points between r_0 and r_L; for $r_L = 0$, 8, 8·8 cm respectively. P_F is zero at $r = r_c$, is proportional to q, and for a constant q follows logarithmic curves such as *a*, *b* and *c*. The curves *a*, *b* and *c* in Fig. 1 are for the value of q appropriate to each r_L when $P_F = P_c$ at $r = r_0$. $(P_c - P_F)$ represents the residual pressure, or manometric head, at any point on the fluid within the cake at $r_c < r < r_0$, and is zero at the cloth-cake interface, where the liquid is assumed at atmospheric pressure with the cloth running "empty."

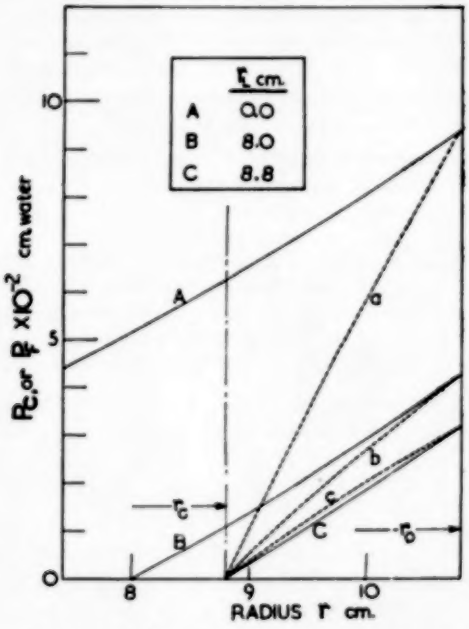

Fig. 1. Variation of P_c and P_F within a cake of uniform permeability at $n' = 1{,}200$ r.p.m., with different r_L.

In Fig. 2 $(P_c - P_F)$ is plotted against r. From both figures it is seen that $(P_c - P_F)$ is positive within the cake for $r_L = 0$ or 8·0 cm, and is negative throughout the cake when $r_L = r_c$, the liquid in the cake pores then being under a pressure lower than atmospheric. Fig. 3 represents this case on a large scale for a thick cake in the 9 in. diameter hydroextractor at the upper limit of speed in the present investigations, which corresponds to the maximum centrifugal fields used in practice. The maximum suction head developed is 150 cm water. As the distribution of actual K variations and the presence

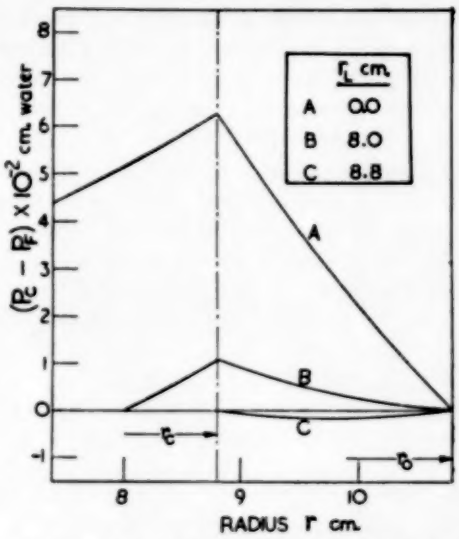

Fig. 2. Variation of $(P_c - P_F)$ within a cake of uniform permeability at $n' = 1{,}200$ r.p.m., with different r_L.

of R tend to reduce this head, it seems likely that the maximum suction head developed in a hydroextractor cake in aqueous liquor is about 150 cm water. This manometric head is not low enough to cause boiling

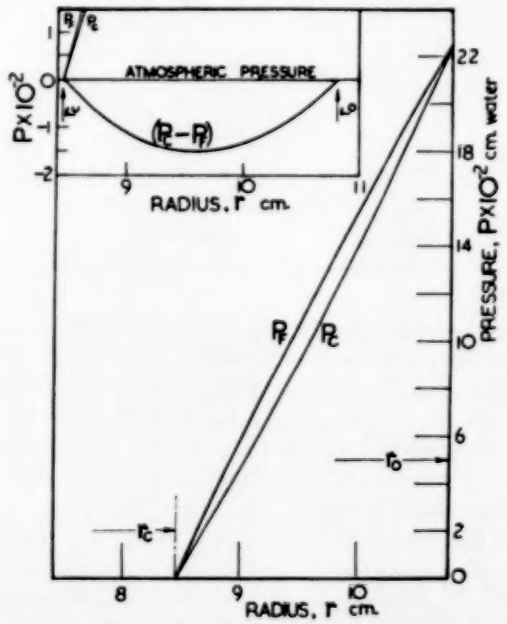

Fig. 3. Variation of P_c and P_F within a cake of uniform permeability at $n' = 3{,}000$ r.p.m., $r_L = r_c = 8{\cdot}46$ cm.

of water within the cake at atmospheric temperatures and hence there is no possibility for a vapour discontinuity in the liquid which would invalidate the proposed flow equations.

When r_L is considerably less than r_c, $(P_c - P_F)$ will be positive throughout the cake, but as r_L increases, a pressure lower than atmospheric is obtained at the outer part of the cake, as in Fig. 4, extending progressively inwards as r_L tends to r_c.

If the P_F curve in Fig. 3 is recalculated taking into consideration the radial change in permeability [2] from inner to outer layers of the cake as 1·25 : 1, the curve approximately coincides with P_c. With a further resistance to flow, R, at the cloth-cake interface, the P_F curve lies below that for P_c at all r

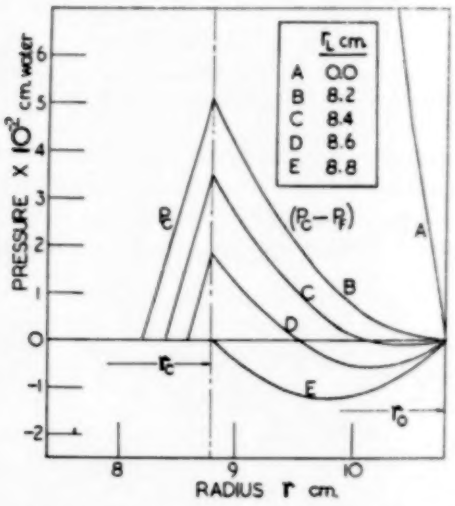

Fig. 4. Variation of $(P_c - P_F)$ within a cake of uniform permeability at $n' = 3{,}000$ r.p.m., with different r_L.

values between r_c and r_0. It is thus highly improbable in practice that any part of a hydroextractor cake will be under sub-atmospheric pressure. It is thus improbable that either vapour or air bubbles will be produced from the liquid within the cake to cause discontinuity in the liquid and hence in the pressure distributions.

In the derivation of equation (1) it was assumed that the cloth layer behind the cake is not filled with liquid and hence does not affect the process of hydroextraction. The earlier study of layer permeability [2] provided a technique for assessing the effect of such a layer of highly permeable material forming part of a hydroextractor cake.

Experimental Technique

In a 9 in. dia. perforated basket centrifuge, one twill and one duck weave cloth layers were used as the support for the cakes. The cloths were spun wet at the highest speed before forming the cake. The cake material was fed to the basket as a thin aqueous slurry, the basket spinning at low speed. The surface of the cake was gently disturbed under water to help the formation of a vertical surface. This was followed by running the submerged cake for one minute at a high speed (2,000 r.p.m.). [4] Drainage time tests were done by measuring the time required for the liquid layer within the cake to move from r_{L1} to r_{L2} at a specified basket speed (mainly 1,050 r.p.m. in this work). The probe arrangement [2] (Fig. 1) was used in

(continued on the opposite page)

Table 1. *Layer Cakes.*

(a) *In hydroextractor basket* :

2. 200 K + (100 K) to 700 K.
1. 300 S + (100 S) to 1,100 S.
3. 200 K + (100 S) to 700 S.
4. 300 S + (100 S) to 700 S, + (100 K) to 300 K.
5. 350 S + 200 K + 100 S + 100 S + 150 S.
6. 350 S + 100 K + 200 S + 150 S.
7. 350 S + 300 K + 200 S + 150 S.
8. 200 S + 200 K + (100 S) to 500 S.

(b) *In small spinning cell* :

9. 2 K + (2 K) to 10 K.
10. 5 C + (1 C) to 9 C.
11. 2·5 C + 4 K + 2·5 C.
12. 3 C + 4 K + 2 C.
13. 4 C + 4 K + 1 C.
14. 5 C + 0·5 K.
15. 5 C + 2 K.
16. 5 C + 4 K.
17. 2 K + 5 C.
18. 4 K + 5 C.
19. 6 K + 5 C.
20. 2·5 C + G + 2·5 C.
21. 4 C + G + 1 C.
22. 5 C + G.

In this table numbers refer to weight of air-dried material in gm and capital letters refer to the material ; K = kieselguhr, S = maize starch, C = chalk, G = gap. Bracketed terms refer to layer increments, e.g. cake No. 4 was composed of an initial 300 *g* starch, sith cakes formed by 100 *g* starch increments up to a total of 700 *g* starch, followed by 100 *g* kieselguhr layers up to a total of 300 *g* kieselguhr. The test series thus included flow measurements on eight cakes, the final form being named cake No. 4. Cake No. 11 was composed of three layers only. The cake No. 20 included a gap between the chalk layers, whereas cake No. 22 had the gap support resting on the single chalk layer.

VOL. 2 1953

determining r_c, r_{L1} and r_{L2}. Keeping the basket speed constant, another mass of slurry was added to form a new layer on the cake. By repeating the sequence, multi-layer cakes were made and their mean permeabilities determined.

Layers were formed from two materials having a wide difference in permeability ; maize starch with a mean permeability of about 3×10^{-7} g/sec.^{2} and kieselguhr with K about 4×10^{-6} g/sec.^{2} The radial position of the higher permeability layer was varied from being the outermost, innermost or middle layer between starch layers of different thicknesses.

Table 1a specifies the different cakes. Cake No. 4 was initially a 300 g starch cake, then a layer of 100 g starch was added, the new 400 g cake being tested. Further cakes were made by 100 g additions up to 700 g starch. This was followed by a layer of 100 g of kieselguhr on the starch cake, the composite cake then being tested. This progressive addition of kieselguhr was followed up to a total of 300 g kieselguhr. After testing every final cake, samples were removed using an annular cutter, and the samples tested for filtration permeability in a $1\frac{1}{2}$ in. diameter filter cell [3]. Samples were cut at different positions of the cake and mean values of permeability are reported. The sample permeabilities were always within 2% of their mean.

The overall mean hydroextraction permeability was calculated from :

$$t = \frac{\mu \cdot g \cdot \log_e \frac{r_0}{r_c}}{4\mu^2 n^2 K_{cm}} \log_e \frac{r_0^2 - r_{L1}^2}{r_0^2 - r_{L2}^2} \qquad (5)$$

$$= C_1 \log_e (r_0/r_c)/K_{cm} \qquad (5a)$$

where C_1 will be a constant for tests at constant μ, n, r_0, r_{L1}, r_{L2}.

The mean filtration permeability was estimated from the following equation for the outflow time t_F for volume V through a cake under a constant head H with inlet at a pressure slightly above atmospheric :

$$t_F = \frac{\mu L V}{AHK_{Fm}} \qquad (6)$$

A series of banded cakes was also formed and tested in a small filter cell which could be attached to the hydroextractor [3]. The layers were always formed by filtration under a suction head of 73 cm Hg and were tested for hydroextraction and filtration permeabilities. Table 1b specifies these cakes. In cakes Nos. 12, 13 and 14 a *Perspex* diaphragm was introduced to form a gap between the existing layer and a new layer to be added. The diaphragm consisted of two discs, with perforations similar to the cell base, separated by three thin short rods. Two filter papers were introduced on the outer sides of the discs. With this diaphragm the effect could be studied of having a 1·2 cm wide gap separating the cake into two layers.

The materials used in the small cell experiments were chalk of approximate permeability $4{\cdot}7 \times 10^{-7}$ g/sec.^{2} and kieselguhr with a permeability about ten times that of the chalk. During hydroextraction tests on this cell, the cake surface at $r = r_c$ was protected by glass wool.]3]

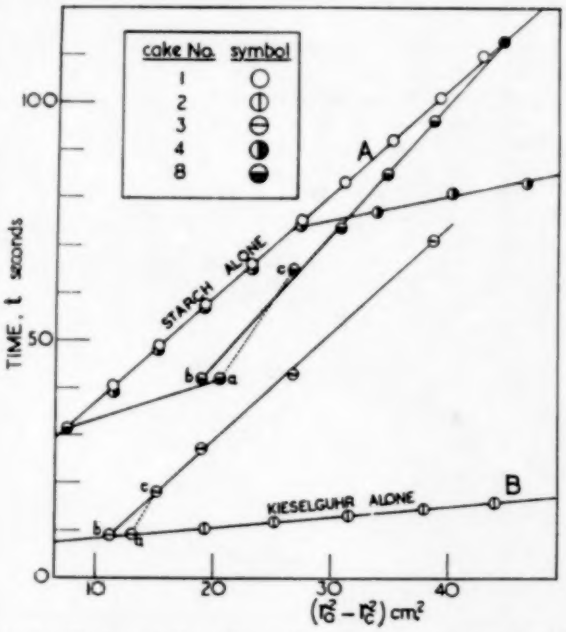

Fig. 5a. Representation of equation (7) for homogeneous and banded cakes.

Discussion of Results

The linear relation found (5) between the drainage time, t, from equation (5) and either $(r_0^2 - r_c^2)$ or the mass of cake W, still held for the multilayer cakes in the 9 in. diameter hydroextractor. Lines A and B in Fig. 5 represent total-starch or total kieselguhr cakes respectively. During the formation of banded cakes, the first layers of one material always followed the appropriate line, illustrating the reproducibility of the results.

In cake No. 4 (Table 1a and Fig. 5a), line *A* was reproduced up to the 700 g starch used ; then the part representing the kieselguhr layers was linear but not parallel to B.

The test on the initial 200 g kieselguhr layer in cake No. 3 is represented by point *a* on line *B* in Fig. 5a. When a thin layer of starch was added, point *c* was obtained, followed by the other points for this cake as further starch layers were added. The line *ac* was steeper than the succeeding line, the decrease in the overall permeability being more than that expected from a calculated mean for 100 g starch

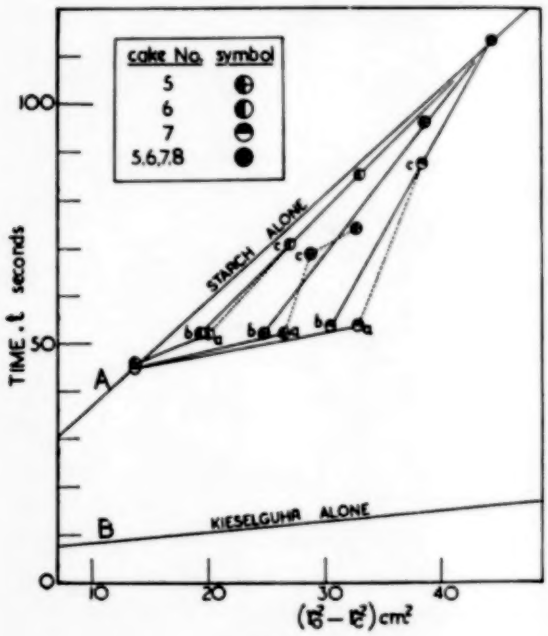

Fig. 5b.

addition to a 200 g kieselguhr cake. Point *a* is based on the value of $(r_0^2 - r_c^2)$ from r_c for a kieselguhr cake alone ([2], Fig. 3, curve *B*). If the layer is covered by a layer of starch, its thickness is reduced and a lower value of $(r_0^2 - r_c^2)$ obtained for the same kieselguhr mass ([2], Fig. 3, curve *C*). If the reduced $(r_0^2 - r_c^2)$ value for the compressed kieselguhr is taken as abscissa, the point *a* in Fig. 5a is moved to point *b*. The adjusted point *b* lies on the full line which is nearly parallel to line *A*. The same phenomenon was noticed in cakes Nos. 5, 6, 7 and 8 ; the effect on the permeability represented by the ordinate in Fig. 5 of the first layer of starch added to the kieselguhr cake was more than that expected for the increment in thickness represented by the abscissa, due to the compression effect associated with it. In each case the point *b* represents the point *a* moved to a radius equivalent to a kieselguhr layer below starch [2].

The condition represented by :

$$t = C\,(r_0^2 - r_c^2 + Y) \qquad (7)$$

was valid for additions within a band of one material, but the value of *C* varied from those for homogeneous

Table 2. The value of C *in equation* (7).

Cake No.	*Layer*	*C.*
2	Kieselguhr alone	4·48
	Kieselguhr on starch :	
6	100 K on 350 S	1·08
5	200 K on 350 S	1·92
7	300 K on 350 S	2·28
8	200 K on 200 S	1·28
4	300 K on 700 S	2·08
1	Starch alone	0·448
	Starch on kieselguhr :	
3	700 S on 200 K	0·44
8	500 S on 200 K on 200 S	0·36
6	350 S on 100 K on 350 S	0·40
5	350 S on 200 K on 350 S	0·312
7	350 S on 300 K on 350 S	0·232

cakes of the particular layer material (Table II). From equations (5) and (7)

$$K = \frac{C_1}{C} \cdot \frac{\log_e \frac{r_0}{r_c}}{r_0^2 - r_c^2 + Y} \qquad (8)$$

whence an increase in *C* indicates an appropriate decrease in *K*. Thus kieselguhr exhibited a lower permeability when it formed a layer between starch layers than when it was alone. The decrease in permeability was greater for thinner kieselguhr layers than for thicker layers.

All lines for the second layer of starch drawn from points *b* tend to meet at a point on line *A* where $r_c = 8{\cdot}5$ cm (Fig. 5), i.e. the overall mean permeabilities of a cake $r_0 = 10{\cdot}8$ and $r_c = 8{\cdot}5$ was the same whether it was formed completely of starch or contained a middle layer of kieselguhr, regardless of either the position or the thickness of the kieselguhr layer. This suggests the necessity of a more detailed

VOL. 2 1953

study of these results to find out whether the middle layers of higher permeability were running full of water.

The overall mean permeability of all tested cakes was less than that calculated as K_m from :

$$\frac{\log_e \frac{r_0}{r_c}}{K_m} = \frac{\log_e \frac{r_0}{r_1}}{K_1} + \frac{\log_e \frac{r_1}{r_2}}{K_2} + \ldots + \frac{\log_e \frac{r_{n-1}}{r_n}}{K_n} \quad (9)$$

For a cake such as the final cake No. 4 the general equation (9) applies with $n = 2$. The dimensions $(r_0 - r_1)$ of the outer starch layer (700 g) and $(r_1 - r_2)$ of the kieselguhr layer (300 g) were measured. The permeability K_1 of the starch layer was measured after the cake had been spun at a speed higher than the test speed. This value corresponded to that shown on curve *B* of Fig. 10 in [2] and included the cloth-caek interface resistance *R*. The double-layer cake with 300 g kieselguhr added was tested after compression at high speed and gave a mean permeability $K_{cm} = 5{\cdot}70 \times 10^{-7}$ (Table 3). A permeability K_2 for

Table 3. Comparison of estimated and measured mean permeabilities for banded cakes.

Cake No.	Mean Permeability, ($K \times 10^7$ g/sec.^{2})	
	K_m calculated from equation (9)	Experimental K_{cm}
3	5·36	4·85
4	5·93	5·70
5	4·90	4·13
6	4·04	3·69
7	5·27	3·94
8	4·90	3·94

the kieselguhr layer was assumed to be the same as that for a layer of the same dimensions and radial position in a cake of kieselguhr alone. This value was derived from mean data given in Table 4 of [2] by the application of equation (9). Using K_2 and K_1 in equation (9), the calculated mean permeability $K_m = 5{\cdot}93 \times 10^{-7}$ was obtained. The slight difference between K_{cm} and K_m justifies the assumption that the outer layer permeability remains constant when covered by inner layers, when all cakes are compressed initially at a speed higher than test speeds.

For a three layer cake such as cake No. 6 the general equation (9) applies with $n = 3$. The dimensions r_0, r_1, r_2, r_3 were measured. Permeability K_1 of the initial layer was measured and assumed constant thereafter. Permeabilities K_2 and K_3 were deduced from previous data [2] as described above. The calculated mean K_m and the measured permeability K_{cm} for the banded cakes are given in Table III.

The differences between K_m and K_{cm} for cakes 3, 5, 6, 7, 8 may indicate that either the banded cakes offered more resistance than expected from equation (9), or that the flow through the kieselguhr layer was discontinuous and hence the centrifugal head developed across them was less than that to be expected from equation (3).

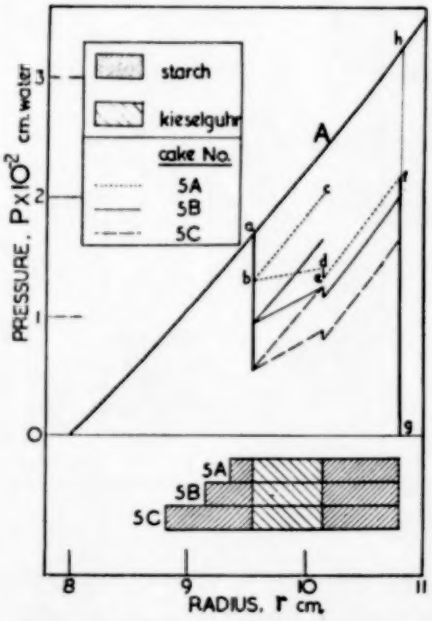

Figs. 6, 7, 8. Pressure distribut'on within banded cakes in the hydroextractor, with $n' = 1{,}050$ r.p.m. and $r_L = 8{\cdot}0$ cm.

Using the layer permeabilities K_2, K_3 derived as for insertion in equation (9) and the measured permeability K_1 of the first layer of a banded cake, the friction head P_f from $r = r_c$ to $r = r$ at any radial position in the cake could be found from equation (4). The values are represented in Figs. 6, 7 and 8. The P_c line *A* gives the centrifugal head developed up to any radius within the liquid, when $r_L = 8{\cdot}0$ cm.

Taking cake No. 5a (Fig. 6) as an example, the point *a* represents the head developed up to the back of the innermost starch layer; the vertical line *ab* represents the frictional head, P_F, dissipated across this inner layer of starch. The line *bc* represents the centrifugal head developed in the kieselguhr layer and is parallel to the P_c line for the same radial positions, assuming that this layer was running full. As the pressure at the back of the cake at $r = r_0$ is assumed to be atmospheric, so *fg* will represent P_F across the outer starch layer. The variation of P_c given by *ef* must be parallel to line *A*, assuming that this starch layer runs full, *e* being at the inner radius of the outermost layer.

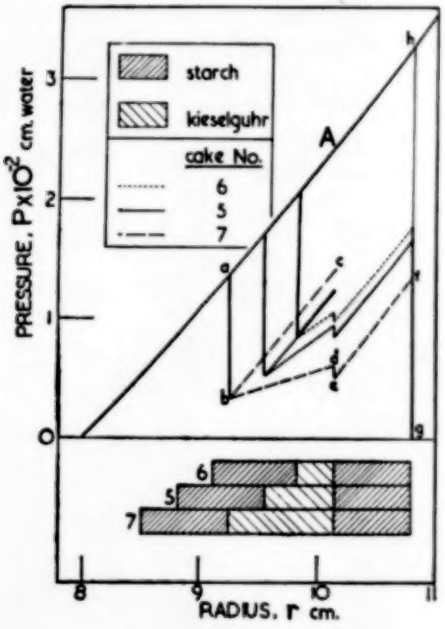

Fig. 7.

The pressure drop across the kieselguhr estimated from K_2 and the known flow rate q is *ed*. If all three layers were running full the friction heads should sum to $ab + ed + fg = hg$. The head *hg* is not accounted for, a considerable discrepancy *cd* being found in each case. The explanation is presumed to be that the cake is not running full at all radii. Cakes of one material conform to equations based on the continuous development of P_c in line *A* at all positions (Fig. 1, 2, 3), the outermost layer resistance is enhanced by the effect of the cloth interface, and the kieselguhr is ten times as permeable as starch. The kieselguhr layer was probably not running full and was thus not developing P_c comparable to line *A*, while the void space in both starch layers was completely filled with liquid. The development of a head *bd* within the kieselguhr layer is discussed later together with the results in Fig. 14. The same phenomenon was noticed in all cakes where a kieselguhr layer existed between layers of starch (Figs. 6, 7 and 8). The discrepancy *cd* was larger with thicker layers of kieselguhr (Fig. 7).

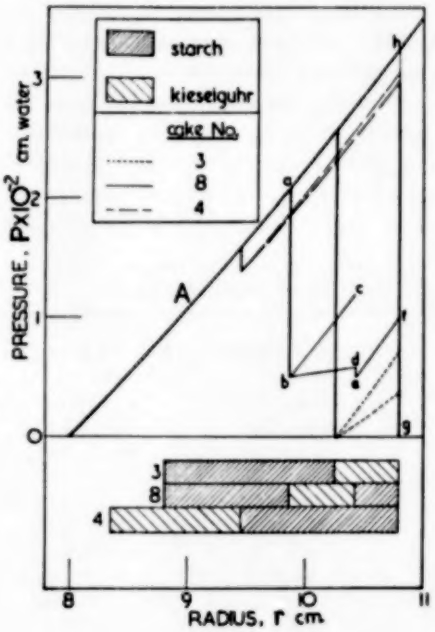

Fig. 8

For cake No. 4, where kieselguhr formed the innermost layer, the calculated friction head added together to approximately the centrifugal head developed, giving very small discrepancy *cd* (Fig. 8). When the kieselguhr formed the outer layer (cake No. 3), the pressure at the outer surface of the starch was atmospheric, indicating that the kieselguhr layer was not running full of liquid (Fig. 8).

Samples were cut from these cakes and tested for filtration, giving the results in Table 4. It was not possible to cut samples from cakes made from kieselguhr alone. It was assumed that the mean filtration

Table 4. Filtration tests on samples of banded cakes from hydroextractor.

Cake No.	$K_{Fm} \times 10^7$	$K_F \times 10^7$ *for kieselguhr*
1	3·75	—
3	6·38	−73
4	6·3	41·5
5	5·2	42
6	4·57	43
7	5·82	39
8	5·0	38

permeability for starch of $3{\cdot}75 \times 10^{-7}$ g/sec.² found from cake No. 1 was the mean permeability in all the other starch layers in succeeding cakes. The permeability of the kieselguhr layer given in the last column of Table 4 was calculated from the relation

$$\frac{r_0 - r_c}{K_{Fm}} \equiv \frac{r_0 - r_1}{K_1} + \frac{r_1 - r_2}{K_2} + \ldots + \frac{r_{n-1} - r_n}{K_n} \quad (10)$$

The calculation K_F for kieselguhr was very near the permeability $K_c = 46{\cdot}0 \times 10^{-7}$ for inner layers of kieselguhr in the hydroextractor. This suggests that in filtration all layers of banded cakes run full, except the bottom layer, if this is of highly permeable material. In the case of cake No. 3, the calculated K_F for kieselguhr was negative, showing that the permeability assigned to the starch layer was low. When the mean K_c of inner layers of starch ($K_c = 4{\cdot}6 \times 10^{-7}$) was assumed to represent K_F for the starch layer, K_F for kieselguhr was found to be infinite, the kieselguhr layer in cake No. 3 apparently offering no resistance to flow. This is consistent with the filtration head being dissipated across the starch layer, the liquid only running through some of the pores of the kieselguhr under the gravitational field. This supports the earlier assumption [3] that the highly permeable cloth runs empty in all the hydroextraction and filtration tests. The result also confirmed the existence of a resistance at the cloth-cake interface. The mean filtration permeability was $3{\cdot}75 \times 10^{-7}$ whenever the starch was adjacent to cloth, for starch layers not in contact with cloth the mean was $4{\cdot}6 \times 10^{-7}$ g/sec.² The difference was due to the inclusion of the cloth-

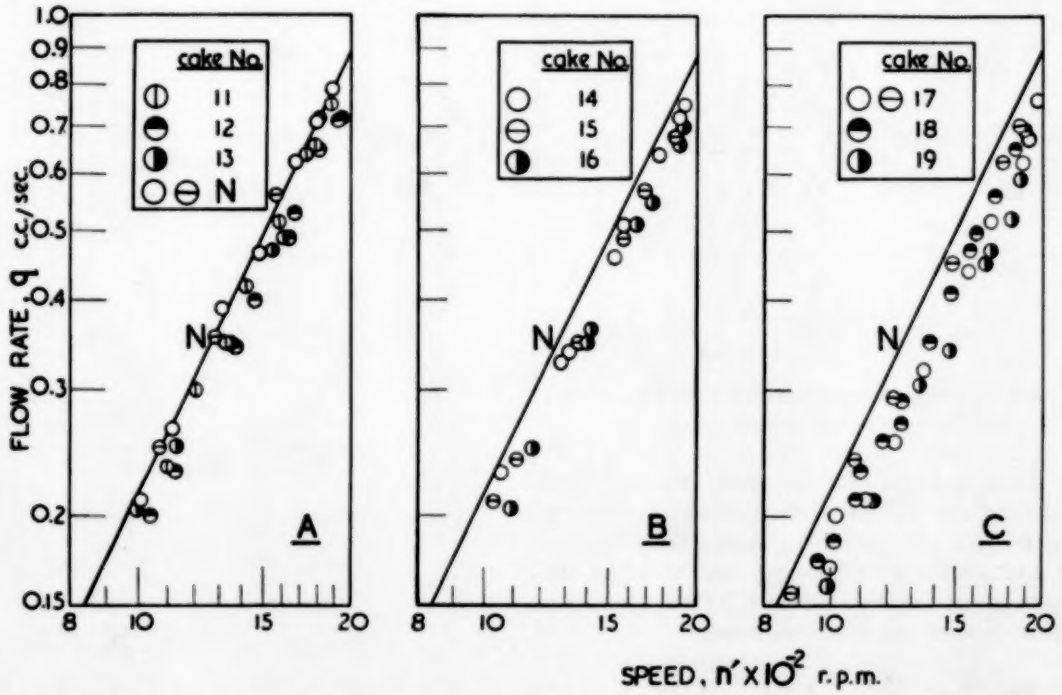

Fig. 9. Relation between rate of flow and speed of revolution for banded cakes. Line *N* is for the 5 *g* chalk cake data in *A*.

starch interface resistance R in the nominal resistance of the starch layer adjacent to cloth.

Tests in the Small Spinning Cell

When cakes in Table 1b were tested for the characteristic q, n data [3] it was found that banded cakes still followed the relation derived for a homogeneous cake :

$$q = \frac{2\pi^2 n^2 A K}{\mu g} \cdot \frac{r_0^2}{(r_0 - r_c)} \qquad (11)$$

The logarithmic q, n plot was a straight line of slope nearly 2·0 for all banded cakes (Fig. 9) and the overall mean permeability was independent of speed. The

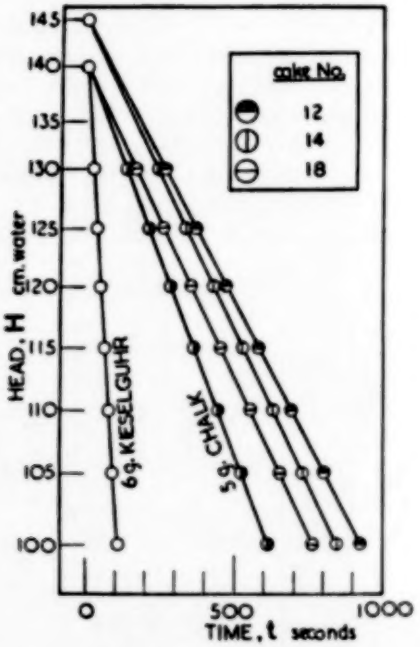

Fig. 10. The application of equation (12) in testing representative banded and homogeneous cakes.

plot of log H against t_p for filtration under a falling positive head with discharge at atmospheric pressure was linear (Fig. 10), satisfying again the filtration equation (12) derived for homogeneous cakes, for the time t_p required for the head to fall from H_1 to H_2 in a stand-pipe of cross sectional area a

$$\log_e \frac{H_1}{H_2} = \frac{K_p \cdot A \cdot t_p}{\mu \cdot a \cdot (r_0 - r_c)} \qquad (12)$$

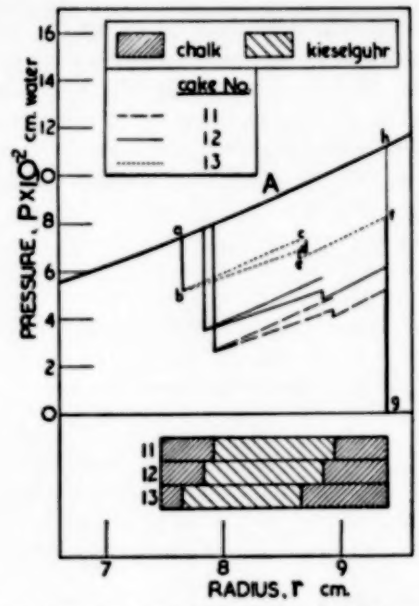

Figs. 11, 12. Pressure distribution within banded cakes in the small spinning cell, with $n' = 1{,}500$ r.p.m. and $r_L = 0$.

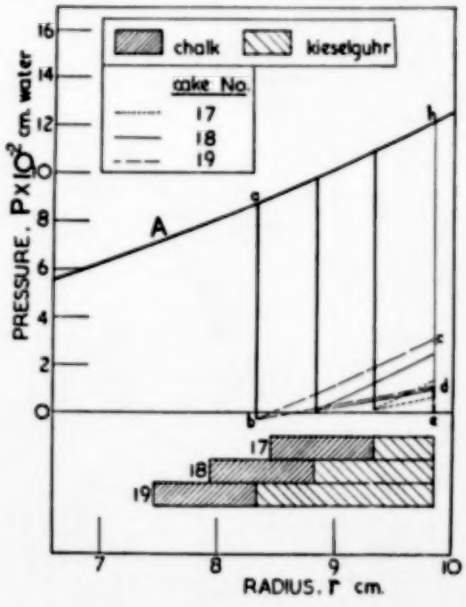

Fig. 12.

From hydroextraction tests on the chalk and kieselguhr used in these experiments, the layer permeability and cloth-cake interface resistance were calculated.

The friction head across each of the layers in a banded cake was found and plotted in Figs. 11, 12. From Fig. 11, the mean discrepancy *cd* forms 3·4% of the total P_c, which could be explained on the assumption that the highly permeable middle layer was not running full. When kieselguhr formed the outer layer (Fig. 12) the pressure at the back of the chalk was atmospheric giving another example of a layer of kieselguhr running empty. The calculated friction loss across such layers *de* is much less than the expected centrifugal force *ce*, which could develop if the outer layer was running full of liquid. The discrepancy is again greater for thicker layers of kieselguhr.

The filtration tests for equation (12) were conducted here by subjecting the cake to a falling positive head around 120 cm water, without applying any suction under the cake. The time t_F for the head to fall from H_1 to H_2 was found and the mean overall filtration permeabilities calculated from equation (12)

Table 5. Filtration tests on banded-cakes in small spinning cell.

Cake No.	$K_{Fm} \times 10^7$	$K_F \times 10^7$ *for kieselguhr layer*
5 *g* Chalk	4·9	—
11	8·85	32·3
12	8·75	30·3
13	8·7	29·5
14	5·25	10
15	6·95	23
16	9·2	31
17	6·9	29
18	9·12	41·5
19	10·3	30·5

are shown in Table 5. The permeability of the kieselguhr layer was estimated from $K_F = 4{\cdot}9 \times 10^{-7}$ for chalk alone and are given in the last column in Table 5. Apart from the expected differences due to compression stresses of successive layers, the results indicate that the highly porous layer was still running full, even when it formed the layer of the cake discharging to atmosphere.

In the cakes Nos. 20, 21, 22, the light *Perspex* gap support did not cause any appreciable compression when resting on the 5 *g* chalk cake, when tested for *q*, *n* data (Fig. 13). When the gap was used to separate the chalk into two layers as in cakes Nos. 20, 21, line

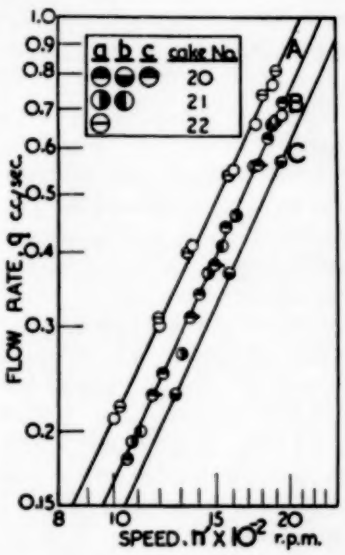

Fig. 13. Relation between flow rate and speed of revolution for cakes separated by a gap.

B in Fig. 13 was obtained. After the test was completed, the liquid feed was stopped and the cake was allowed to run dry for a minute, followed by a rapid

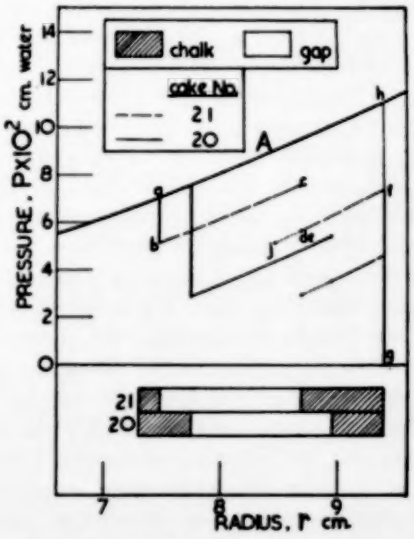

Fig. 14. Pressure distribution within cakes separated by a gap.

test of the q, n condition. With cake No. 21 no difference could be observed between the first rapid test and others taken later, all agreeing with line B. However, in the case of cake No. 20, the first point found quickly after the feed was resumed fell on line C, whereas the other points determined afterwards returned to line B.

When the friction drops across the layers were calculated and plotted in Fig. 14, the gap resistance de being zero, it was found that cd formed 17·5% of the total expected centrifugal head hg. The centrifugal head fd was extrapolated to a point j at the same pressure level as b. An empty compartment of constant pressure probably extends behind the inner layer of cake from the radial position b to position j. The section of the gap from j to d was filled with a layer of liquid maintained in front of the outermost chalk layer. The friction head dissipated in this outer layer was the sum of the centrifugal head developed from j to d in front of the cake, from d to f within the cake, and the pressure differential between the empty compartment and the atmosphere, represented by the ordinate to b.

When the cake was allowed to run dry, the pressure in the gap decreased to atmospheric, as the outer layer emptied, then began to increase when the flow was resumed.

In the case of cake No. 21, the inner layer would allow a flow of 1·53 cc/sec. when running full and discharging to atmosphere at the radial position b, whereas the outer layer would allow 0·22 cc/sec. when a liquid layer extended from position b to $r = r_0$ at g. Due to this great difference, the pressure in the gap would be increased on the resumption of flow and readings showing lower flow rates than line B in Fig. 13 could not be detected. The corresponding values for cake No. 20 are 0·66 and 0·31 cc/sec. respectively, giving an opportunity for a rapid test to detect lower flow rates, as on line C, Fig. 13, when the pressure in the gap was still developing.

Filtration results conforming to equation (12) provided filtration permeabilities given in Table 6. The pressure of the gap support and its filter papers in cake No. 22 had an insignificant effect on permeability. The 6% reduction in permeability with two chalk layers is probably associated with an interface resistance between chalk and filter paper, mainly at the back of the upper chalk layer. The great effect noted in hydroextraction attributed to the gap running empty did not occur in filtration when the filtrate was discharged at atmospheric pressure.

Table 6. Filtration tests in small spinning cell.

Cakes with layers separated by a gap	
Cake No.	$K_p \times 10^7$
5 g Chalk	4·9
20	4·57
21	4·66
22	4·83

Conclusions

The study of hydroextraction and filtration permeabilities of banded cakes has demonstrated that

(i) a backing layer of high permeability material in a hydroextractor does not run full of liquid and the atmospheric pressure is exerted on the outer face of the inner layer of less permeable material. This conclusion based on 10 : 1 ratio of permeabilities is considered to confirm the assumption that a cloth support in the basket does not run full, the corresponding permeability ratio being 50 : 1.

(ii) the given interpretation of the results is in accordance with the previous conclusion that there is a small effect of compression on cake permeability with the present cake materials, and a significant resistance to flow at the cloth-cake interface,

(iii) a highly permeable mid-layer within a cake does not run full of liquid, a constant pressure region existing within this layer,

(iv) the conditions here demonstrated to cause a flow discontinuity within a cake are absent with cakes of one material, and the assumption of continuous centrifugal head development within homogeneous cakes, fundamental to the equations and proposed mechanism of hydroextraction, is supported,

(v) with usual operating conditions, it is improbable that a suction head develops in any region within the cake to form a discontinuity in the assumed flow pattern.

VOL. 2 1953

NOMENCLATURE

A	= cross-sectional area of filter bed	cm^2
a	= cross-sectional area of tube in filtration tests	cm^2
C	= gradient in equation (7)	$sec./cm^2$
g	= gravitational acceleration	$cm./sec.^2$
H	= hydrostatic head in filtration tests H_1, H_2 limits of H.	cm
K	= permeability ; K_1, K_2, . . . K_n for different layers ; K_F for filtration ; K_c for hydroextraction ; K_{Fm}, K_{cm} appropriate experimental means ; K_m calculated mean from K_1, K_2, . . . K_n	$g/sec.^2$
L	= length of filter bed in filtration tests	cm
n	= speed of revolution	rev./sec.
n'	=	rev./min.
P_c	= centrifugal pressure	cm water
P_F	= friction head	cm water
q	= drainage rate through cake	cc/sec
R	= cake-cloth interface resistance	$sec.^2/g$
r	= radius from basket axis (cm); r_0 for cake outer surface ; r_c for cake inner surface ; r_L for liquid inner surface ; r_1, r_2 . . . . r_n for interfaces between cake layers ; r_{L1}, r_{L2} limits of r_L in drainage time equation	
t	= time t_F time in filtration equation	seconds
V	= volume flowing in time t_F in filtration equation	cc
W	= mass of dry solid in cake	g
X	= height of centrifuge basket	cm
μ	= viscosity of liquid	poise

REFERENCES

[1] BURAK, N. and STORROW, J. A.; J. Soc. Chem. Ind. 1950 **69** 8. [2] HARUNI, M. M. and STORROW, J. A.; Hydroextraction IV. Chem. Eng. Sci. 1952 **1** 154. [3] HARUNI, M. M. and STORROW, J. A.; Ind. Eng. Chem., 1952 **44** 2751, [4] INGLESENT, H. and STORROW, J. A.; Ind. Chem. 1951 **27** 76.

Chemical Engineering Science, 1953, Vol. 2, pp. 120 to 126. Pergamon Press Ltd.

Note on the Duhem equation

NORBERT V. IBL
Laboratory of Physical Chemistry, Swiss Federal Institute of Technology, Zürich, Switzerland

BARNETT F. DODGE
Department of Chemical Engineering, Yale University, New Haven, Conn.

(*Received* 19 *March* 1953)

Summary—The conditions of validity of the simple forms of the Gibbs-Duhem equation most commonly used in practice are discussed. A simple derivation is given of the exact relationships valid at p constant (resp. T constant) in the case of a binary vapour-liquid system at equilibrium and connecting together either (a) the fugacities of the components, or (b) the activity coefficients of the components, or (c) the compositions of the vapour and liquid phase with T (resp. p). The application of the general relationships is discussed, especially for the case of a constant pressure, important in distillation problems.

Résumé—Les auteurs discutent les conditions de validité des formes approchées de l'équation de Gibbs-Duhem employées dans la pratique. Sont également discutées les équations exactes valables soit à p constant, soit à T constant, dans le cas d'un système binaire liquide-vapeur en équilibre et reliant entre elles soit : (*a*) les fugacités des constituants ; (*b*) les coefficients d'activité des constituants ; (*c*) les titres des phases gazeuse et liquide en fonction de T ou de p, respectivement.

VOL. 2 1953

The Duhem (or Gibbs-Duhem) equation is commonly applied to binary, liquid-vapour systems at equilibrium and is widely used in the calculation of the composition of the coexisting phases of binary systems important in distillation problems. Two of the most often encountered forms of this equation are

$$\left(\frac{\partial \ln f_1}{\partial \ln x}\right)_{T,p} = \left(\frac{\partial \ln f_2}{\partial \ln (1-x)}\right)_{T,p} \tag{1}$$

and

$$\left(\frac{\partial \ln \gamma_1}{\partial \ln x}\right)_{T,p} = \left(\frac{\partial \ln \gamma_2}{\partial \ln (1-x)}\right)_{T,p} \tag{2}$$

The derivation of these equations, as given for instance by LEWIS and RANDALL [5], restricts their validity to conditions of constant pressure and temperature. In the case of a two-phase system these equations are therefore no longer equilibrium relations, since the phase rule shows that in such a system one cannot have at variable composition both temperature and pressure kept constant and have the equilibrium between the two phases still being maintained. In vapour-liquid calculations, therefore, one of the two conditions (p = const. or T = const.) has to be dropped; eqs. (1) and (2) are then used as strictly isothermal ones, whereas eq. (2) has also been used by BEATTY and CALINGAERT [1] and others at constant p and variable T. Both ways of using eqs. (1) and (2) are only approximations and it is important in a given case to discover if these approximations are admissible or not. This is especially important when eq. (2) is used as an isobaric relation, because then the approximation is often not very good. The object of the present note is to give a review of the general and exact relationships valid at T constant and p variable on the one hand, p constant and T variable on the other, the relations being derived in a simple but rigorous fashion which shows clearly the conditions of validity of the general forms of the Gibbs-Duhem equation as well as that of the more simple relations commonly used in practice.

The thermodynamic potential F of a homogeneous system is a homogeneous function of the first degree in the mole numbers of the components of the system. From Euler's theorem on homogeneous functions follows (for a binary system)

$$F = n_1 \mu_1 + n_2 \mu_2$$

and therefore

$$dF = n_1\,d\mu_1 + n_2\,d\mu_2 + \mu_1\,dn_1 + \mu_2\,dn_2 \qquad (3)$$

On the other hand we have the familiar relation, valid for any open phase :

$$dF = V dp - S dT + \mu_1\,dn_1 + \mu_2\,dn_2 \quad (4)$$

Subtracting (4) from (3) we get

$$V dp - S dT = n_1\,d\mu_1 + n_2\,d\mu_2$$

This is the most general form of the Gibbs equation valid at variable T and p. It may be written as well for the liquid phase as for the vapour phase of a binary two-phase system at equilibrium.

If we divide by the sum of the mole numbers $n_1 + n_2$ and bear in mind that the sum of the mole fractions is 1 we get, for instance for the liquid phase

$$V'_m dp - S'_m dT = x d\mu_1 + (1-x)\,d\mu_2\dagger \qquad (5)$$

At constant temperature and pressure this equation reduces at once to eq. (1), if we take into account the relation between μ and the fugacities

$$d\mu = RT\,d\ln f \qquad \text{at } T \text{ constant.} \quad (6)$$

(a) *Relationships valid at T constant and p variable*

At constant temperature eq. (5) takes the form (if we bear in mind the relation (6))

$$x d\ln f_1 + (1-x) d\ln f_2 = \frac{V'_m}{RT} dp \quad \text{at } T \text{ constant} \quad (7)$$

If we regard x, the mole fraction of component 1, as the main variable we may also write

$$\frac{d\ln f_1}{d\ln x} = \frac{d\ln f_2}{d\ln(1-x)} + \frac{V'_m}{RT}\frac{dp}{dx} \text{ at } T \text{ constant} \quad (8)$$

or

$$\frac{d\ln \bar{p}_1}{d\ln x} = \frac{d\ln \bar{p}_2}{d\ln(1-x)} + \frac{V'_m}{RT}\frac{dp}{dx} \text{ at } T \text{ constant} \quad (9)$$

the latter equation applying when the gas phase is ideal. Eqs. (7) and (8) are exact forms of the Duhem equation which remain strictly valid if we apply them to equilibrium calculations in a two-phase system maintained at constant temperature. Eq. (8) differs from the simple relation (1) by the term $\frac{V'_m}{RT}\frac{dp}{dx}$, where $\frac{dp}{dx}$ is the slope of the curve of the total vapour pressure vs. the composition of the liquid phase (at constant T), and V'_m is the volume of 1 mole of the liquid phase, which may easily be calculated from the density of the solution. It will be possible therefore in a given case to evaluate at least approximately the correction term $\frac{V'_m}{RT}\frac{dp}{dx}$ and thus the degree of accuracy given by the simple relation (1). In general, this latter can be used without significant error if, as is usually the case, the molal volume of the liquid phase is negligible in comparison to that of the vapour phase (this because of the fact that $\frac{x\,d\ln \bar{p}_1}{dx}$ and $\frac{(1-x)\,d\ln \bar{p}_2}{dx}$ are larger or at least of the same order of magnitude as $\frac{d\ln p}{dx}$, which is equal to $\frac{V''_m}{RT}\frac{dp}{dx}$ in the case of an ideal gas phase).†

Equations (8) and (9) give a relation between the partial pressures (resp. the fugacities) of the two components of the mixture. Often, however, one wants a direct relationship between the total pressure p and the compositions x and y of the liquid phase and the vapour phase (that is an equation relating the dew-point line to the bubble-point line). The general form of this p-x-y relationship may be derived as follows.

The fugacity f_1 of the component 1 of the vapour phase is a single-valued function of T, p and y (or $\ln y$). We may therefore calculate the total exact differential of $\ln f_1$ as follows

$$d\ln f_1 = \left(\frac{\partial \ln f_1}{\partial T}\right)_{p,y} dT + \left(\frac{\partial \ln f_1}{\partial p}\right)_{T,y} dp + \left(\frac{\partial \ln f_1}{d\ln y}\right)_{T,p} d\ln y \quad (10)$$

† We do not give a superscript to the variables μ_1, μ_2 p and T since at equilibrium they have the same value in both phases.

† See also footnote, p. 122, column 2.

An analogous relation holds for f_2 :

$$\mathrm{d}\ln f_2 = \left(\frac{\partial \ln f_2}{\partial T}\right)_{p,1-y}\mathrm{d}T + \left(\frac{\partial \ln f_2}{\partial p}\right)_{T,1-y}\mathrm{d}p + \left(\frac{\partial \ln f_2}{\partial \ln(1-y)}\right)_{T,p}\mathrm{d}\ln(1-y) \quad (11)$$

We have also the familiar relations (see for instance [2d], [3b] or [4b]).

$$\left(\frac{\partial \ln f_1}{\partial p}\right)_{T,y} = \frac{\bar{v}_1^{\cdot}}{RT} \quad (12)$$

$$\left(\frac{\partial \ln f_2}{\partial p}\right)_{T,1-y} = \frac{\bar{v}_2^{\cdot}}{RT} \quad (13)$$

where $\bar{v}_1^{\cdot}$ and $\bar{v}_2^{\cdot}$ mean the partial molal volumes of component 1 and 2, respectively.

Furthermore, we may write on the basis of (5) and (6) applied to a single phase at constant T and p

$$\left(\frac{\partial \ln f_1}{\partial \ln y}\right)_{T,p} = \left(\frac{\partial \ln f_2}{\partial \ln(1-y)}\right)_{T,p} \quad (14)$$

At equilibrium the fugacities are the same in both phases. We may therefore replace in eq. (7) $\mathrm{d}\ln f_1$ and $\mathrm{d}\ln f_2$ by their values as given by eqs. (10) and (11) which readily yields (if we bear in mind eqs. (14), (12) and (13) and the fact that the first term of the right-hand side of eqs. (10) and (11) is zero at T constant) :

$$\frac{\mathrm{d}p}{RT} = \frac{y-x}{y(1-y)\,\Delta V}\left(\frac{\partial \ln f_1}{\partial \ln y}\right)_{T,p}\mathrm{d}y \text{ at } T \text{ constant} \quad (15)$$

where ΔV is equal to $x\,\bar{v}_1^{\cdot} + (1-x)\,\bar{v}_2^{\cdot} - V_m'$; it is the increase in volume when 1 mole of the liquid phase is evaporated into such an amount of the equilibrium vapour phase that the composition of the latter is not substantially changed. The partial derivative $\left(\frac{\partial \ln f_1}{\partial \ln y}\right)_{T,p}$ † refers to the vapour phase and means the variation of fugacity of component 1 with composition at constant T and p. Eq. (15) is the exact p-x-y relationship valid at T constant. If the vapour phase is a mixture of ideal gases we have

$$\left(\frac{\partial \ln f_1}{\partial \ln y}\right)_{T,p} = 1 \qquad \bar{v}'' = \frac{RT}{p}$$

If then the volume of the liquid phase is negligibly small, eq. (15) reduces to

$$\frac{\mathrm{d}p}{p} = \frac{y-x}{y(1-y)}\,\mathrm{d}y \qquad \text{at } T \text{ constant} \quad (16)$$

This equation, as well as

$$\left(\frac{\partial \ln \bar{p}_1}{\partial \ln x}\right)_T = \left(\frac{\partial \ln \bar{p}_2}{\partial \ln(1-x)}\right)_T \quad (17)$$

are two of the forms of Duhem's equation, which are most commonly used in practice. They are isothermal relations valid only if : (1) the vapour phase may be considered as a system of ideal gases, (2) the molal volume of the liquid phase is negligible in comparison to that of the vapour phase.† If these conditions are not fulfilled the exact relationships (15) or (8) should be used.

The use of the exact eq. (15) is quite similar to that of eq. (16) (see for instance [2c]). The values of $\bar{v}_1^{\cdot}$, $\bar{v}_2^{\cdot}$ and $\left(\frac{\partial \ln f_1}{\partial \ln y}\right)_{T,p}$ have to be taken from an equation of state of the real gas-mixture. A considerable simplification occurs if we admit as a first approximation the validity of the Lewis-Randall rule

$$f_1 = y f_1^{\bullet} \qquad f_2 = (1-y) f_2^{\bullet}$$

($f_1^{\bullet}, f_2^{\bullet}$ = fugacities of the pure components)

† As has been already pointed out the partial derivative $\left(\frac{\partial \ln f_1}{\partial \ln y}\right)_{T,p}$ does not correspond to changes along the equilibrium line, when the vapour phase is at equilibrium with the liquid phase. It still has, of course, even in this case a perfectly determined value.

† It should be noted that this latter condition does not hold quite in the same way for eq. (16) as for eq. (17). In the case of eq. (16) the relative volume of the liquid phase corresponds exactly to the error involved when using this equation, that is, if the molal volume of the liquid phase is for instance 0·1 % of that of the vapour phase, both sides of eq. (16) will also differ by 0·1 %. Such a simple relation does not hold in the case of eq. (17). In general if the relative volume of the liquid phase is for instance 0·1 % both sides of eq. (17) will also differ by less than 0·1 % or 0·2 %. But if the vapour pressure of one of the pure components of the mixture is much larger (for instance four times larger) than that of the other component a substantially larger error may occur at one of the ends of the diagram, where x or 1-x is small.

VOL. 2 1953

which holds in general with a fair approximation at pseudoreduced pressures less than 0·8 [4c]. $\left(\frac{\partial \ln f_1}{\partial \ln y}\right)_{T,p}$ is now equal to 1 and $\bar{v}_1^*$ and $\bar{v}_2^*$ are equal to the molal volumes of the pure components in the gaseous state at the temperature and pressure of the mixture. They may be evaluated from an equation of state of the pure components (or from a generalized (reduced) compressibility diagram).†

(b) *Relationships valid at p constant and T variable*

As most vaporization operations are conducted at constant pressure and variable temperature this case is of considerable practical importance.

If we write the analogues of eqs. (10) and (11) for the liquid phase we have

$$\mathrm{d}\ln f_1 = \left(\frac{\partial \ln f_1}{\partial p}\right)_{T,x}\mathrm{d}p + \left(\frac{\partial \ln f_1}{\partial T}\right)_{p,x}\mathrm{d}T + \left(\frac{\partial \ln f_1}{\partial \ln x}\right)_{T,p}\mathrm{d}\ln x \quad (18)$$

$$\mathrm{d}\ln f_2 = \left(\frac{\partial \ln f_2}{\partial p}\right)_{T,1-x}\mathrm{d}p + \left(\frac{\partial \ln f_2}{\partial T}\right)_{p,1-x}\mathrm{d}T + \left(\frac{\partial \ln f_2}{\partial \ln (1-x)}\right)_{T,p}\mathrm{d}\ln (1-x) \quad (19)$$

the first term of the right-hand sides of these equations being zero at p constant. Furthermore we have the relations (see for instance [3c])

$$\left(\frac{\partial \ln f_1}{\partial T}\right)_{p,x} = \frac{H_1^* - \bar{H}_1'}{RT^2} \quad (20)$$

$$\left(\frac{\partial \ln f_2}{\partial T}\right)_{p,1-x} = \frac{H_2^* - \bar{H}_2'}{RT^2} \quad (21)$$

where H_1^* and H_2^* are the molal enthalpies of the pure components in the ideal gas state.

† It may happen that one (or both) of the pure gaseous components would be liquefied if it existed alone at the temperature and pressure of the mixture. The equation of state (or the reduced compressibility diagram) has then to be extrapolated into the two-phase region. This procedure will not be very accurate if extended extrapolation is necessary. In general, however, only a rough knowledge of the departure of the vapour phase from ideal behaviour is needed in the use of Duhem's equation.

Combining (20) and (21) we may also write

$$x\left(\frac{\partial \ln f_1}{\partial T}\right)_{p,x} + (1-x)\left(\frac{\partial \ln f_2}{\partial T}\right)_{p,1-x} = \frac{\Delta H}{RT^2} \quad (22)$$

where ΔH means the term $xH_1^* + (1-x)H_2^* - x\bar{H}_1' - (1-x)\bar{H}_2'$ and is therefore the molal ideal heat of vaporization (i.e. the heat required to vaporize 1 mole of the solution, when the pressure of the obtained vapour is sufficiently low for the ideal gas laws to be valid).

Rearranging eqs. (18) and (19) and combining them with eq. (22) we readily get, if we bear in mind that $\left(\frac{\partial \ln f_1}{\partial \ln x}\right)_{T,p}$ and $\left(\frac{\partial \ln f_2}{\partial \ln (1-x)}\right)_{T,p}$ are equal because of Duhem's equation when applied to a single phase at T and p constant

$$\frac{\mathrm{d}\ln f_1}{\mathrm{d}\ln x} = \frac{\mathrm{d}\ln f_2}{\mathrm{d}\ln (1-x)} + \frac{\Delta H}{RT^2}\frac{\mathrm{d}T}{\mathrm{d}x} \text{ at } p \text{ constant} \quad (23)$$

Eq. (23) is an exact form of Duhem's equation valid at constant total pressure and variable temperature. $\frac{\mathrm{d}T}{\mathrm{d}x}$ is the slope of the curve T vs. x at p constant (boiling point line). ΔH may be evaluated from the heat of mixing (corresponding to the composition x of the solution at the considered point of the diagram) and the ideal heats of vaporization of the pure components. In most cases the heat of vaporization is large in comparison to the heat of mixing, so that this latter needs often to be known only roughly or may even be neglected.

It should be noted that at constant pressure the simple eq. (1) cannot be used even as an approximation. This can be seen in the following way.

If we assume the gas-phase to be ideal we have

$$f_1 = yp \qquad f_2 = (1-y)\,p$$

If we then neglect the term $\frac{\Delta H}{RT^2}\frac{\mathrm{d}T}{\mathrm{d}x}$ eq. (23) may be put into the form

$$\frac{x-y}{y(1-y)} = 0$$

which relation obviously does not hold even approximately.

Eq. (23) relates the curves of the fugacities – or in the case of an ideal gas phase, of the partial vapour pressures – of the two components with the composition of the liquid mixture, when the total pressure is kept constant. In isobaric problems, however, equations relating directly the boiling point line to the dew-point line are often more useful. The exact T-x-y relationship may be simply obtained as follows. At p constant the second term of the right-hand side of eqs. (10) and (11) is zero. If we replace in eq. (23) $\mathrm{d} \ln f_1$ and $\mathrm{d} \ln f_2$ by the values given by eqs. (10) and (11), noting that $\left(\frac{\partial \ln f_1}{\partial \ln y}\right)_{T,p}$ and $\left(\frac{\partial \ln f_2}{\partial \ln (1-y)}\right)_{T,p}$ are equal, we get

$$\left[\frac{\Delta H}{RT^2} - x\left(\frac{\partial \ln f_1}{\partial T}\right)_{p,y} - (1-x)\left(\frac{\partial \ln f_2}{\partial T}\right)_{p,1-y}\right] \mathrm{d}T = \left(\frac{\partial \ln f_1}{\partial \ln y}\right)_{T,p} \frac{x-y}{y(1-y)} \mathrm{d}y \quad \text{at } p \text{ constant} \quad (24)$$

The terms $\left(\frac{\partial \ln f_1}{\partial T}\right)_{p,y}$, $\left(\frac{\partial \ln f_2}{\partial T}\right)_{p,1-y}$ and $\left(\frac{\partial \ln f_1}{\partial \ln y}\right)_{T,p}$ refer to the vapour phase : they are the corrections for the imperfection of the vapour ; the first two are equal to zero and the third to unity when the vapour phase is a mixture of ideal gases. In this case eq. (24) reduces to

$$\frac{\mathrm{d}T}{RT^2} = \frac{x-y}{y(1-y)\,\Delta H} \mathrm{d}y \quad \text{at } p \text{ constant} \quad (25)$$

which is at p constant the analogue of eq. (16).

Eqs. (25) or (24) may be used to check the consistency of experimentally determined vapour-liquid boundary curves in a way quite similar to that † employed when applying eq. (16). The most accurate method is to integrate to determine T (the righthand side of eq. (25), and in the case of eq. (24) both sides of the equation, have to be integrated graphically).†† A further possibility is to calculate the value of $\frac{\mathrm{d}T}{\mathrm{d}y}$ from eq. (25) or (24) and compare it with the slope of the dew-point line. Other possible applications of eqs. (24) and (25) are the calculation of the boiling-point line, if only the dew-point line is known, or the evaluation of the heat of mixing (and thus of the enthalpy of the liquid mixture) from the T-x-y diagram and the heats of vaporization of the pure components.

When the departure of the gas phase from ideal behaviour cannot be neglected, eq. (24) has to be used. The correction terms for the imperfection of the vapour have to be evaluated from an equation of state of the real gas mixture. A considerable simplification arises if we assume the validity of the Lewis-Randall rule. $\left(\frac{\partial \ln f_1}{\partial \ln y}\right)_{T,p}$ is then equal to 1 and the two other correction terms are given by

$$\left(\frac{\partial \ln f_1}{\partial T}\right)_{p,y} = \frac{H_1^\circ - H_1^{\circ\bullet}}{RT^2} \text{ and } \left(\frac{\partial \ln f_2}{\partial T}\right)_{p,1-y} = \frac{H_2^\circ - H_2^{\circ\bullet}}{RT^2}$$

where H_1° and H_2° are the molal enthalpies of the pure components in the ideal gas-state whereas $H_1^{\circ\bullet}$ and $H_2^{\circ\bullet}$ are the molal enthalpies of the pure gaseous components at the temperature and pressure of the mixture. These correction terms may be calculated in the usual way from the equations of state of the pure components (see for instance [2a], [3a], [4a]), or from the generalized (reduced) enthalpy-diagrams (see for instance [2b]).†

(c) *General forms of Duhem's equation in terms of activity coefficients*

If we choose as the standard states the pure liquid components at the pressure and temperature of the solution, the activity coefficients are given by

$$\gamma_1 = \frac{f_1}{x f_1^\bullet} \qquad \gamma_2 = \frac{f_2}{(1-x) f_2^\bullet}$$

where $f_1^\bullet$ and $f_2^\bullet$ are the fugacities of the pure liquids at the same pressure and temperature as the mixture. If we introduce these values into equation (8) we readily obtain

$$\frac{\mathrm{d} \ln \gamma_1}{\mathrm{d} \ln x} + \frac{x\,\mathrm{d} \ln f_1^\bullet}{\mathrm{d}p} \frac{\mathrm{d}p}{\mathrm{d}x} = \frac{\mathrm{d} \ln \gamma_2}{\mathrm{d} \ln (1-x)} - \frac{(1-x)\,\mathrm{d} \ln f_2^\bullet}{\mathrm{d}p} \frac{\mathrm{d}p}{\mathrm{d}x} + \frac{V_m'}{RT} \frac{\mathrm{d}p}{\mathrm{d}x} \quad \text{at } T \text{ constant}$$

† The use of eq. (16) is given for instance by DODGE [2c].

†† The way of evaluating ΔH has already been discussed.

† See also footnote, p. 123.

VOL. 2 1953

or

$$\frac{\mathrm{d}\ln\gamma_1}{\mathrm{d}\ln x} = \frac{\mathrm{d}\ln\gamma_2}{\mathrm{d}\ln(1-x)} + \left[V'_m - x\,V'^{\bullet}_1 - (1-x)\,V'^{\bullet}_2\right]\frac{1}{RT}\cdot\frac{\mathrm{d}p}{\mathrm{d}x} \quad \text{at } T \text{ constant} \quad (26)$$

where $V'^{\bullet}_1$ and $V'^{\bullet}_2$ mean the molal volumes of the pure liquids at the pressure and the temperature of the mixture, and the term $V'_m - xV'^{\bullet}_1 - (1-x)V'^{\bullet}_2$ is therefore the volume change accompanying the mixing (per mole of mixture). We will denote the second term on the right-hand side of (26) by the letter A.

Similarly, we obtain from eq. (23)

$$\frac{\mathrm{d}\ln\gamma_1}{\mathrm{d}\ln x} + \frac{x\,\mathrm{d}\ln f^{\bullet}_1}{\mathrm{d}T}\frac{\mathrm{d}T}{\mathrm{d}x} = \frac{\mathrm{d}\ln\gamma_2}{\mathrm{d}\ln(1-x)} - \frac{(1-x)\,\mathrm{d}\ln f^{\bullet}_2}{\mathrm{d}T}\frac{\mathrm{d}T}{\mathrm{d}x} + \left[x\,H'^{\circ}_1 + (1-x)\,H'^{\circ}_2 - x\,\overline{H}'_1 - (1-x)\,\overline{H}'_2\right]\frac{1}{RT^2}\frac{\mathrm{d}T}{\mathrm{d}x} \quad \text{at } p \text{ constant}$$

or

$$\frac{\mathrm{d}\ln\gamma_1}{\mathrm{d}\ln x} = \frac{\mathrm{d}\ln\gamma_2}{\mathrm{d}\ln(1-x)} - \left[x\,\overline{H}'_1 + (1-x)\,\overline{H}'_2 - x\,H'^{\bullet}_1 - (1-x)\,H'^{\bullet}_2\right]\frac{1}{RT^2}\frac{\mathrm{d}T}{\mathrm{d}x} \quad \text{at } p \text{ constant} \quad (27)$$

where the term $x\overline{H}'_1 + (1-x)\,\overline{H}'_2 - xH'^{\bullet}_1 - (1-x)\,H'^{\bullet}_2$ is the integral heat of mixing (per mole of mixture).† We will denote the second term on the right-hand side of (27) by the letter B.

(26) and (27) are the exact equations relating together at T and p constant, respectively, the curves of γ_1 and γ_2 vs. x. The approximate equation (2) may therefore be used (a) at T constant when the correction term A is negligible, (b) at p constant when the term B is negligibly small in comparison to $\frac{\mathrm{d}\ln\gamma_1}{\mathrm{d}\ln x}$. The first condition is mostly fulfilled (except perhaps at high temperatures and pressures where $\frac{\mathrm{d}p}{\mathrm{d}x}$ and the volume may be large) and eq. (2) will in general hold at T constant with a high degree of accuracy. It is not so, however, at p constant. In this case before using the simple relation (2) the term B (which depends on the steepness of the boiling point curve and the heat of mixing) should always be evaluated at least approximately and compared to $\frac{\mathrm{d}\ln\gamma_1}{\mathrm{d}\ln x}$. It should be noted that at p constant the simple relation (2) might hold fairly well in certain parts of the diagram and still be in serious error at other values of x.

Let us take as example the system acetone-carbon disulfide studied by various authors [6], [7], [8] at $t = 35{\cdot}2°$ and $p = 760$ mm (BEATTY and CALINGAERT [1] have applied eq. (2) to this system, to check the values obtained at T constant as well as those measured at p constant). At $x = 0{\cdot}5$, $\frac{\mathrm{d}p}{\mathrm{d}x}$ is about 0·13 atm., and the volume changes by about 1·4% when the components are mixed [7], which gives for A a value of 5×10^{-6}. $\frac{\mathrm{d}\ln\gamma_1}{\mathrm{d}\ln x}$ being ca. 0·7, it follows that at T constant both sides of eq. (2) differ only by 0·0007%. Again at $x = 0{\cdot}5$ the heat of mixing is 330 cal/mole [7], $\frac{\mathrm{d}T}{\mathrm{d}x}$ is about 3·5° and B is then equal to 0·005. At p constant both sides of eq. (2) differ therefore by 0·7% when $x = 0{\cdot}5$. The same calculation for $x = 0{\cdot}9$ and $x = 0{\cdot}1$ reveals that the degree of accuracy given by eq. (2) is now rather poor since B is not less than 7% and 13% of $\frac{\mathrm{d}\ln\gamma_1}{\mathrm{d}\ln x}$, respectively.

† Strictly speaking this heat of mixing (as well as the volume effect of the mixing) should be measured at the pressure and the temperature corresponding to the composition x of the considered point of the curves γ_1 and γ_2 vs. x. The available experimental values will however in general correspond to another pressure than that of the considered mixture (this also because of the fact that the standard state as defined above may be a hypothetical one). This will however involve no appreciable error in the evaluation of the correction terms A and B. As these last values will need most often to be known only approximately it will often even be sufficient to know the heat of mixing and volume change at another temperature than that of the mixture (for instance at room temperature).

NOTATION

f = fugacity
F = thermodynamic potential ($= H - TS$)
H = enthalpy
$\bar{H}$ = partial molal enthalpy
ΔH = ideal heat of vaporization (per mole of mixture)
n = number of moles
p = total pressure
$\bar{p}$ = partial pressure
R = ideal gas constant
S = total entropy of a phase
S_m = molal entropy (entropy of a mole of the mixture)
T = thermodynamic temperature
V = total volume of a phase
V_m = molal volume (volume of a mole of the mixture)
$\bar{v}$ = partial molal volume
x = mole fraction of component 1 in the liquid phase
y = mole fraction of component 1 in the vapour phase
μ = chemical potential (partial molal thermodynamic potential)
γ = activity coefficient

Subscripts : 1 and 2 refer to component 1 and 2, respectively.

Superscripts : $'$ and $''$ refer to the liquid and vapour phase, respectively ; $^\circ$ refers to the standard state of low pressure, where gases are ideal ; $^\bullet$ refers to a pure component.

REFERENCES

[1] BEATTY, H. A. and CALINGAERT, G.; Ind. Eng. Chem. 1934 **26** 904. [2] DODGE, B. F.; Chemical Engineering Thermodynamics 1944 (a) p. 218 (b) p. 241 (c) p. 557 (d) p. 124. [3] GLASSTONE, S.; Thermodynamics for chemists 1947 (a) p. 160 (b) p. 265 (c) p. 266. [4] HOUGEN, O. A. and WATSON, K. M.; Chemical Process Principles, Part II 1947 (a) p. 493 (b) p. 625 (c) p. 626. [5] LEWIS, G. N. and RANDALL, M.; Thermodynamics 1923 p. 43. [6] ROSANOFF, M. A. and EASLEY, C. W.; J. Amer. Chem. Soc. 1909 **31** 953. [7] SCHMIDT, G. C.; Z. physik. Ch. 1926 **121** 221. [8] ZAWIDZKI, J. v.; Z. physik. Ch. 1900 **35** 129.

VOL. 2 1953

Chemical Engineering Science, 1953, Vol. 2, pp. 127 to 138 Pergamon Press Ltd.

The condensation of vapour from gas-vapour mixtures

R. C. CAIRNS

School of Chemical Engineering, New South Wales University of Technology, Broadway, Sydney, Australia

(*Received* 23 *December* 1952)

Summary—The accepted methods for the design of condensers to handle gas-vapour mixtures are reviewed and a single verticle tube condenser is described from which data are obtained for the systems chloroform and air, and steam and air.

The method of COLBURN and HOUGEN [4] is applied to a run on each of the systems and the calculated area compared with the expected area. The approximate method of COLBURN [3] is also applied to the same runs and the area obtained again compared with the expected area.

The area required to cool a saturated mixture of chloroform and air from 120·2°F to 94·0°F calculated by the CHOLBURN and HOUGEN [4] method is found to be in good agreement with the expected area, being within 2% of it. The method applied to the cooling of a saturated mixture of steam and air from 168·3°F to 129·9°F gives an area which also agrees well, being within 5% of that expected.

The modification of the COLBURN and HOUGEN [4] method suggested by SMITH [10] is found unnecessary in the cases studied.

The approximate design procedure proposed by COLBURN [3], applied to the same conditions, is found to give an area approximately 40% greater than expected for both systems.

Résumé—L'auteur passe en revue les méthodes classiques de calcul pour les condenseurs traitant des mélanges de gaz et vapeurs. Il décrit un condenseur à tube vertical unique utilisé pour l'étude des systèmes air-chloroforme et air-vapeur d'eau : Les résultats expérimentaux sont comparés avec ceux prédits par les méthodes classiques.

Dans le cas de $CHCl_3$—air, (condensation entre 120·2°F et 94·0°F), la méthode de COLBURN—HOUGEN [4] concorde à 20% près. Dans le cas H_2O—air (condensation entre 168·3°F et 129·9°F) la concordance atteint environ 5%.

La modification apportée par SMITH [10] à la méthode précédente n'est pas nécessaire dans les deux cas étudiés.

La méthode de calcul approximatif proposée par COLBURN [3] prévoit les surfaces en excès de 40%, dans les deux cas étudiés.

INTRODUCTION

When a gas-vapour mixture is exposed to a surface at a lower temperature than the dew point of the mixture, condensation of the vapour occurs. A gas film is formed at the surface, which contains a higher gas concentration than the main stream.

COLBURN and HOUGEN [4] have shown that the diffusion of the vapour molecules through the gas film plays an important part in the transfer of heat from the gas-vapour mixture. They presented a design procedure for estimating the surface area required for a cooler-condenser, to cool a saturated gas-vapour mixture, along the saturation line.

In their treatment, at any particular point in the condenser, the quantity of heat flowing per unit time per unit cross-sectional area through the resistances of the condensate layer, the metal wall, scale and cooling water film is made equal to the heat flow through the gas film. The heat flow through the gas film is made up of sensible heat lost by the mixture and latent heat transferred as the vapour diffuses through the gas film and condenses in the condensate film. The total heat flow is represented by an overall coefficient U, multiplied by the temperature drop from the mixture to the water.

These conditions are represented by :

$$h_g (t_g - t_c) + K M_v \lambda (p_v - p_c) = h_o (t_c - t_w) = U \Delta t \qquad (1)$$

or in words, the heat flow to the condensate surface is equal to the heat flow from the

condensate surface and these are each equal to $U\Delta t$.

At any value of t_g in the condenser, all the variables in equation (1) are known or can be calculated, except t_c, p_c and U. The value of p_c follows if t_c is known and the value of $U\Delta t$ is obtained by a trial and error substitution of several values of t_c until the desired equality is obtained.

By choosing six or more temperatures for t_g and applying this procedure the point values of $U\Delta t$ can be evaluated and graphical integration of equation (2) is possible, since values of $U\Delta t$ are known for increments of the total heat transferred.

$$A = \int \frac{dq}{U\Delta t} \qquad (2)$$

The method presented by COLBURN and HOUGEN is accepted by all texts at the present time, but it is often pointed out that the method as applied is extremely tedious. There also appears to be no experimental evidence in the literature to support the design procedure. SMITH [10], however, does state that considerably higher heat transfer rates than expected were obtained on equipment designed by this method.

SMITH attributes this to the method of calculating the heat transferred between points. This is made up of the heat of condensation and the heat transferred by the cooling of the gas, the uncondensed vapour and the condensate. To calculate the latter of these it is assumed that the condensate is at the same temperature as the main stream, which is not strictly true. Heat is removed by the cooling water as the condensate flows past the cooling surface and the condensate must be at a lower temperature than the mixture.

Where the latent heat of vaporisation is small, SMITH suggests that the heat transferred by the cooling of the condensate is no longer negligible, as it is in the example worked out by COLBURN and HOUGEN, and for organic vapour and gas mixtures some allowance must be made.

SMITH gives a modification of the COLBURN and HOUGEN method whereby an estimate is made of the final condensate temperature from the empirical equation :

$$\left(\frac{t_a - t_w}{t_g - t_w}\right)_{\substack{COLD\\END}} = 0{\cdot}2 \qquad (3)$$

From this t_a is found and the total heat transferred from inlet to outlet, is calculated, using t_a as the condensate temperature, not t_g. A plot of the terminal values of t_c and t_w versus q is made and for a calculated value of t_w, the estimated true t_a is obtained by interpolation on this graph. The corrected heat transferred and corrected t_w are then found and this new value of t_w used in equation (1) to solve for t_c by trial and error as before.

SILVER [9] gives approximate methods for different types of cooler condensers for estimating the gas film sensible heat transfer coefficient and the mean overall heat transfer coefficient.

The calculations necessitate knowing the area of an existing condenser and its operating terminal conditions. Conversely the methods are applicable to the estimation of the surface area if the gas film sensible heat transfer coefficients are known.

The methods are based on the assumption that h_s is constant throughout the cooling process and that the ratio of the sensible heat transfer coefficient to the total gas film heat transfer coefficient is equal to the ratio of the sensible heat capacity change to the total heat capacity change.

However the calculation of the area required for a given set of conditions does not appear possible where the values of h_s are not known for various equipment under different operating conditions, or where it is not possible to assume h_s is constant. This may occur where there is a large velocity change of the gas-vapour mixture in the equipment caused by the removal of vapour from high concentrations of the vapour in the mixture.

COLBURN [3] recently has presented an approximate design method which involves only the terminal conditions of the condenser and eliminates the need for point to point heat balances and the trial and error calculation in order to obtain $U\Delta t$. In this method the overall driving force from mixture to cooling water is expressed as an enthalpy difference $(i_g - i_w^*)$, and the conductance of heat is expressed as an overall

VOL. 2 1953

coefficient per unit enthalpy difference $\left(\frac{U_s}{c_s}\right)$ such that :

$$dq/dA = \left(U_s/c_s\right)(i_g - i_w^*) \qquad (4)$$

COLBURN finds $\left(U_s/c_s\right)$ from equation (5) :

$$1/\left(U_s/c_s\right) = 1/\left(h_s/c_s\right) + 1/\left(h_o/m\right) \qquad (5)$$

and he evaluates m, for the purposes of calculation at t_g.

Assuming $\left(U_s/c_s\right)$ constant, then equation (4) becomes :

$$A = \frac{q}{\left(U_s/c_s\right)(\Delta i)_{lm}} \qquad (6)$$

The value of $\left(U_s/c_s\right)$ however is known to vary and the arithmetic average of the top and bottom values of $\left(U_s/c_s\right)$ is used to evaluate A.

Although the mechanism of the condensation of a vapour from a non-condensing gas is well understood, little appears to have been done to check experimentally the methods just described. It was felt that an experimental investigation on the validity of the design methods was most desirable. It is the purpose of this paper to present experimental data, obtained from a simple apparatus, to which design calculations can be applied and to compare the accuracy of the design methods with the known surface area used in the experimental work.

Air mixtures with pure chloroform and with water vapour were chosen for the experimental work because of the differences in properties of these two vapours; notably the latent heat of vaporization.

APPARATUS AND PROCEDURE

The apparatus, as shown in Fig. 1 consists principally of a boiler, a gas-vapour mixer, a verticle tube condenser, a condensate separator and an auxiliary condenser.

The boiler is made from 1/16 in. steel sheet,

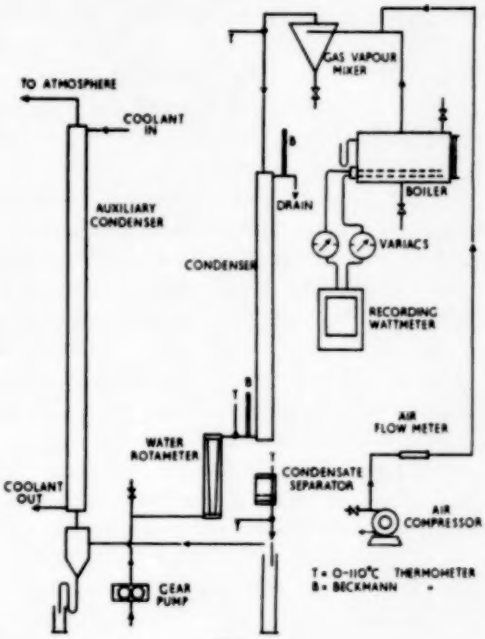

Fig. 1.

and the internal dimensions are 10 in. × 10 in. × 16 in. The boiler is cadmium plated and is fitted with a gauge glass and safety lute. A ¼ in. filling cock is provided and the exit vapour line leaves from an approximately 1 in. I.D. copper tube in the centre of the cover plate. A 3,000 watt *Helicoil A.G.E.*, twin element immersion heater is sealed into the side of the boiler. The power input to the boiler is controlled by a 9 amps 280 volt Variac on each element and is recorded on an *Evershed and Vignoles* Recording Watt Meter.

The vapour lines from the boiler are approximately 1 in. I.D. and lead to the gas-vapour mixer which is also in glass. One foot before the mixer the air is introduced through a ¼ in. glass line pointing in the direction of the vapour flow and the gas plus vapour enter the mixer tangentially. The mixer is constructed on the lines of a cyclone separator, the mixture of gas and vapour leaving from the top of the mixer. The mixed gas and vapour then pass to the condenser in approximately 1 in. glass lines; a three feet calming section is provided before the condenser.

The condenser consists of a verticle double-pipe exchanger, with the gas-vapour mixture flowing

downwards inside the centre tube and cooling water flowing countercurrent to this in the annulus. The centre tube is of standard 12 gauge copper and is 1·289 in. O.D., 1·081 in. I.D. and the length of tube exposed to cooling water is six feet (or 1·70 sq. ft. internal area).

The join between glass calming section and copper tube is a simple butt joint, both surfaces being first ground flat. The internal diameter of the glass at the join is the same as that of the copper tube. The two sections are held together by means of a bored rubber bung which fits into the annulus between the two metal tubes. The external tube forming the water jacket is standard 8 gauge black iron pipe 2·055 in. I.D.

A 1 in. I.D., glass line which is six inches long leads from the bottom of the condenser and is fitted to the condenser in a similar manner to the calming section. The condensate formed is separated from the exit gas-vapour mixture in the condensate separator. This is attached to the glass line which is flared at its end. Another glass line fitting under this takes off the exit gas-vapour mixture. The condensate rate is determined directly from the volume collected in a known time.

For the chloroform and air runs, an auxiliary condenser was used to remove as much chloroform vapour as possible before discharging to the atmosphere. A nine feet condenser with trichlorethylene cooled by dry-ice as the coolant, was used for this purpose.

The maximum cooling water-rate available was pumped by a gear pump and metered through a rotameter.

Standard thermometers are located at the top of the calming section, at the condensate outlet of the separator, in the exit gas-vapour line and in the inlet water line. Beckmann thermometers are used at the inlet and outlet of the cooling water to determine the water temperature rise. No correction was found necessary, at the water-rate used, to allow for fluid friction.

For the system, chloroform and air, where the ratio of vapour to air is very high, the air was pumped by an Edwards Type IV Compressor ($\frac{1}{4}$ hp 1 kg/sq. cm., 75 litres/min.) and measured through a calibrated constriction meter before entering the system. For the steam and air runs a *Beecox* Rotary Air Pump, 0-10 c.f.m., was used for the higher air rates needed in this case. The air was first filtered and metered through a previously checked $\frac{1}{2}$ in. × $\frac{1}{4}$ in. Venturi. For this system also the air was electrically heated before entering the vapour line.

The boiler was calibrated for power input versus rate of evaporation for both water and chloroform. This calibration was obtained by setting the equipment for total condensation without air flow and after allowing sufficient time

VOL. 2 1953

Table 1

System	*Run*	*Vapour Rate lbs/ hour*	*Air rate lbs/ hour*	*Cooling water rate lbs/ hour*	*Gas-Vapour temperature °C*				*Water inlet temp. °C*	*Water temp. rise °C*	*Condensate temp. °C*	*Condensate lbs/ hour*	*Heat in / Heat out*
					Inlet		*Outlet*						
					Exptl.	*Calcd.*	*Exptl.*	*Calcd.*					
Chloroform and air	1	47·2	5·80	2010	51·8	49·0	36·3	34·4	13·7	1·14	30·0	32·3	0·94
	2	47·2	5·80	2010	51·0	49·0	36·3	35·0	15·0	1·12	30·0	31·8	0·94
	3	47·2	5·80	2010	51·4	49·0	36·4	34·4	14·9	1·12	30·0	32·3	0·95
	4	47·2	5·80	2010	51·3	49·0	36·3	34·4	14·7	1·11	30·0	32·4	0·96
Steam and air	1	10·1	24·3	2010	74·8	76·3	52·5	55·9	17·7	2·26	34·0	7·22	0·98
	2	10·2	25·5	2010	75·0	75·7	52·9	55·0	18·2	2·33	35·0	7·32	0·96
	3	10·0	25·5	2010	74·6	75·4	52·5	54·0	19·0	2·29	35·0	7·25	0·97
	4	10·0	25·2	2010	75·0	75·7	53·0	54·4	19·1	2·26	34·5	7·27	0·99

for the equilibrium the condensate rate was measured. A voltage regulator was found necessary to reduce the effects of mains voltage fluctuation.

The boiler is lagged with a 1 in. asbestos sheeting and the condenser is lagged with 1½ in. asbestos rope. All glass lines and the gas-vapour mixer is lagged with 3 in. of slag wool.

The chloroform used was fractionated from B.P. chloroform to remove the added alcohol and then dried. The water used was taken directly from the mains.

In making a run the water was turned on and the boiler set at the required vaporisation rate. Sufficient time was allowed for the vaporisation from the boiler to become steady and the air was introduced into the vapour line. The apparatus was allowed to come to equilibrium and before readings were taken the mixer was drained. The amount of condensate in the mixer after a run was found to be negligible. The time required to make a run was approximately two hours.

The results for both systems are listed in Table 1 together with the calculated saturation temperatures at inlet and outlet and the ratio of heat in to heat out, obtained by an enthalpy balance applied to the experimental results.

Applied Calculations

The design method of Colburn and Hougen [4] and also that of Colburn [3] were applied to one set of experimental results from each system. Run numbers 4 in each case were chosen for the calculations.

In applying the design methods the inlet temperature at saturation corresponding to the humidity of the inlet mixture was used for the purpose of the calculation and the outlet saturation temperature corresponding to the calculated humidity of the outlet mixture was also used. This was necessitated by the fact that the experimental temperatures did not correspond exactly to the temperature at saturation for the humidity involved, and that the Colburn and Hougen method assumes cooling along the saturation line. In view of the fact that the actual temperatures did not differ greatly from the theoretical temperatures as seen in Table 1, this procedure is justifiable.

The calculations for both systems have been carried through simultaneously and for the sake of clarity sample calculations are given :

Colburn and Hougen Method

Table 2 lists the conditions known for each system

Table 2

	Chloroform and air	*Steam and air*
Air rate lb moles/hour	0·20	0·869
Inlet temperature °F	120·2	168·3
Outlet temperature °F	94·0	129·9
Cooling water rate lbs/hour	2010	2010
Inlet water temperature °C	14·7	19·1
Pressure atm	1	1
Inlet conditions :		
Vapour pressure atm	0·664	0·391
Gas partial pressure atm	0·336	0·609
Outlet conditions :		
Vapour pressure atm	0·382	0·151
Gas partial pressure atm	0·618	0·849
lb moles vapour entering per hour	0·395	0·558
lb moles vapour leaving per hour	0·124	0·155
lb moles vapour condensed per hour	0·271	0·403

and the results of the overall mass balances. The inlet and outlet vapour pressures are obtained at the inlet and outlet temperatures respectively.

Throughout the calculations the following properties were taken as constant :

c for air	0·24 B.T.U./(lb)(°F)
c for water vapour	0·45 B.T.U./(lb)(°F)
c for chloroform vapour	0·14 B.T.U./(lb)(°F)
c for water	1·0 B.T.U./(lb)(°F)
c for chloroform liquid	0·23 B.T.U./(lb)(°F)
Molecular weight of air	29
Molecular weight of chloroform	119·4
Molecular weight of water	18

The physical properties of the gas-vapour mixtures are given in Table 3 and were evaluated at the point temperatures chosen. The viscosities of the mixtures were calculated using the method of Bromley and Wilke [1] while the molecular weights, densities and specific heats were calculated by standard methods. The diffusivities

Table 3

System	*Point*	*Gas-Vapour temp. °F*	*Vapour pressure atm*	*Viscosity lb/(hr) (ft)*	*Molecular Weight*	*Density lb/cft*	*Specific heat BTU/(lb) (°F)*	*Diffusivity ft²/hour*	*Schmidt No.*
Chloroform and air	(1)	120·2	0·664	0·0293	89·0	0·210	0·174	0·356	0·394
	(2)	115·0	0·600	0·0305	83·2	0·198	0·180	0·351	0·439
	(3)	110·0	0·543	0·0310	78·1	0·188	0·186	0·346	0·476
	(4)	105·0	0·489	0·0317	73·2	0·178	0·191	0·342	0·521
	(5)	100·0	0·440	0·0322	68·7	0·168	0·196	0·337	0·569
	(6)	94·0	0·382	0·0329	63·5	0·157	0·201	0·332	0·631
Steam and air	(1)	168·3	0·391	0·0407	24·7	0·0539	0·322	1·23	0·61
	(2)	160·0	0·322	0·0419	25·5	0·0563	0·308	1·20	0·62
	(3)	150·0	0·254	0·0430	26·2	0·0588	0·293	1·17	0·63
	(4)	140·0	0·197	0·0439	26·8	0·0612	0·282	1·14	0·63
	(5)	135·0	0·172	0·0443	27·1	0·0624	0·276	1·13	0·63
	(6)	129·9	0·151	0·0445	27·3	0·0634	0·272	1·12	0·63

were found from the equation of GILLILAND [5] for chloroform and air but the value for the diffusivity reported by SHERWOOD [8] for steam and air was used after correcting for temperature. The Schmidt numbers were calculated but since the variation for steam and air was slight an

Table 4

System	*Points*	*Heat of condensation B.T.U./hour*	*Heat removed from condensate B.T.U./hour*	*Heat removed from vapour B.T.U./hour*	*Heat removed from air B.T.U./hour*	*Total B.T.U./hour*
Chloroform and air	(1)-(2)	1225	13·6	26·1	7·2	1272
	(2)-(3)	803	21·6	19·8	7·0	851
	(3)-(4)	611	28·0	15·9	7·0	662
	(4)-(5)	444	32·7	13·1	7·0	497
	(5)-(6)	433	44·7	12·4	8·4	499
	Totals	3516	140·6	87·4	36·6	3781
Steam and air	(1)-(2)	2602	21·7	27·8	50·2	2702
	(2)-(3)	2110	47·2	24·0	60·5	2242
	(3)-(4)	1506	62·1	17·3	60·5	1646
	(4)-(5)	584	33·9	7·3	30·2	655
	(5)-(6)	476	37·0	6·4	30·8	550
	Totals	7278	201·9	82·8	232·2	7795

VOL. 2 1953

average value of 0·62 was chosen for calculating the mass transfer coefficient.

In Table 4 the results of the point to point heat balances are shown.

e.g. Points (4)-(5) *Steam and Air*

Heat of condensation

$$=0{\cdot}869\times\left(\frac{0{\cdot}197}{0{\cdot}803}-\frac{0{\cdot}172}{0{\cdot}828}\right)18\times 1014 = 384 \text{ B.T.U./hr}$$

Heat removed from condensate (condensed assumed to leave at same temperature as the mixture)

$$=0{\cdot}869\times\left(\frac{0{\cdot}391}{0{\cdot}609}-\frac{0{\cdot}172}{0{\cdot}828}\right)18\times 5 = 33{\cdot}9 \text{ B.T.U./hr}$$

Heat removed fron uncondensed vapour

$$=\frac{0{\cdot}172}{0{\cdot}828}\times 0{\cdot}869\times 18\times 0{\cdot}45\times 5 = 7{\cdot}3 \text{ B.T.U./hr}$$

Heat removed fron air

$$=0{\cdot}869\times 29\times 0{\cdot}24\times 5 = 30{\cdot}2 \text{ B.T.U./hr}$$

Heat transferred between points (4) and (5) ——————

655 B.T.U./hr

The total heat transferred between inlet and outlet is thus 3781 B.T.U./hr for the chloroform and air system and 7795 B.T.U./hr for steam and air. This enables the water temperature at each point and the total water temperature rise to be calculated. Table 5 gives these values.

The mass velocities and Reynolds numbers are

Table 5.

System	*Points*	*Total heat transferred B.T.U./hour*	*Water temp. change °F*	*Water temp. °F*
Chloroform and air	At (1)	0	0	60·3
	(1)-(2)	1272	0·63	59·7
	(2)-(3)	851	0·42	59·3
	(3)-(4)	662	0·33	59·0
	(4)-(5)	497	0·25	58·7
	(5)-(6)	499	0·25	58·5
	Totals	3782	1·88	
Steam and air	At (1)	0	0	70·3
	(1)-(2)	2702	1·34	68·9
	(2)-(3)	2242	1·12	67·8
	(3)-(4)	1646	0·82	67·0
	(4) -(5)	655	0·33	66·6
	(4)-(6)	550	0·27	66·4
	Totals	7795	3·88	

Table 6

System	*Point*	G	N_{Re}	j	h_g	$K\times p_{gf}$	h_c
Chloroform and air	(1)	8,310	25,400	0·0032	5·37	0·556	0
	(2)	6,530	19,300	0·0033	4·50	0·448	311
	(3)	5,370	15,600	0·0035	4·05	0·394	263
	(4)	4,490	12,800	0·0037	3·68	0·351	241
	(5)	3,850	10,800	0·0039	3·42	0·318	229
	(6)	3,240	8,900	0·0040	3·02	0·277	219
Steam and air	(1)	5,530	12,200	0·0038	8·13	1·17	1360
	(2)	5,120	11,000	0·0039	7·38	1·08	1360
	(3)	4,790	10,000	0·0040	6·74	1·01	1360
	(4)	4,560	9,400	0·0040	6·17	0·935	1360
	(5)	4,470	9,100	0·0040	5·92	0·906	1360
	(6)	4,390	8,900	0·0040	5·74	0·886	1360

shown in Table 6 for each point. These are evaluated as follows :

e.g. Point (2). *Chloroform and Air*

Tube diameter = 1·081 in.

Cross-sectional area = 0·00637 sq. ft.

$$G = \frac{0{\cdot}20\,(119{\cdot}4 \times \frac{0{\cdot}600}{0{\cdot}400} + 29)}{0{\cdot}00637}$$

$$= 6{,}530 \text{ lb/(hr) (sq ft)}$$

and μ at (2) = 0·0305 lb/(hr) (ft)

So $N_{Re} = \frac{1{\cdot}081 \times 6530}{12 \times 0{\cdot}0305} = 19300$

The j factor is read directly from figure (1) of reference [2].

The values of the sensible heat transfer coefficient, h_s, and the mass transfer coefficient, K, are calculated from the equations of CHILTON and COLBURN [2].

$$h_s = \frac{j\,c\,G}{\left(\frac{c\mu}{k}\right)^{\frac{2}{3}}} \qquad (7)$$

$$K = \frac{j\,G}{M_m\,p_{gf}\left(\frac{\mu}{\rho\,D}\right)^{\frac{2}{3}}} \qquad (8)$$

The value of 0·80 is assumed for the Prandtl number for chloroform and air giving

$$(\mathrm{Pr})^{\frac{2}{3}} = 0{\cdot}862$$

For steam and air a value of 0·76 is taken for the Prandtl number giving

$$(\mathrm{Pr})^{\frac{2}{3}} = 0{\cdot}833$$

The calculated values of h_s and $(K \times p_{gf})$ are also listed in Table 6.

e.g. Point (2). *Chloroform and air.*

$j = 0{\cdot}0033$ $\quad G = 6530$

$c = 0{\cdot}180$ $\quad \left(\frac{c\mu}{k}\right)^{\frac{2}{3}} = 0{\cdot}862$

From equation (7),

$$h_s = \frac{0{\cdot}0033 \times 0{\cdot}180 \times 6530}{0{\cdot}862}$$

$$= 4{\cdot}50 \text{ B.T.U./(hr) (sq ft) (°F)}$$

Also $M_m = 83{\cdot}2$

$$\frac{\mu}{\rho D} = 0{\cdot}439$$

From equation (8),

$$K = \frac{0{\cdot}0033 \times 6530}{83{\cdot}2 \times p_{gf} \times (0{\cdot}439)^{\frac{2}{3}}}$$

$$= \frac{0{\cdot}448}{p_{gf}}$$

Heat Transfer Coefficients other than the Gas Film

The heat that is transferred to the surface of the condensate film must pass through the resistances of the condensate film, the tube wall, scale and the water film before being removed by the cooling water. These resistances are calculated as follows :

(a) *Condensate film, h_c*

Values of h_c are calculated from the equation of NUSSELT [6],

$$h_c = 0{\cdot}93\,k\left(\frac{\rho\,g_L}{\mu\,\Gamma}\right)^{\frac{1}{3}} \qquad (9)$$

For chloroform and air h_c was calculated at each point. For steam and air, where the condensing film coefficient is much higher, the value at the bottom of the condenser, where the resistance is greatest, was taken as constant throughout the condenser. This value was calculated from equation (9) as 1360 B.T.U./(hr) (sq ft) (°F). Table 6 also lists the point values of h_c for chloroform.

(b) *Tube Wall, h_p*

$$h_m = \frac{220 \times 12}{0{\cdot}104}$$

$$= 25{,}400 \text{ B.T.U./(hr) (sq ft) (°F)}$$

(c) *Scale, h_d*

A scale coefficient of 1,000 is allowed for both systems.

$$h_d = 1{,}000 \text{ B.T.U./(hr) (sq ft) (°F)}$$

(d) *Water Film, h_w*

The film coefficient on the water side was evaluated from COLBURN's equation for fluids inside tubes in turbulent flow, recommended by PERRY [7] for turbulent flow in an annulus :

$$\left(\frac{h_w}{cG}\right)\left(\frac{c\,\mu_f}{k}\right)^{\frac{2}{3}} = 0{\cdot}023\left(\frac{d_e G}{\mu f}\right)^{-0{\cdot}2} \qquad (10)$$

The value obtained is

$$h_w = 179 \text{ B.T.U./(hr) (sq ft) (°F)}$$

When these coefficients are corrected to the inside area of the condenser tube,

$$h_a = 179 \text{ B.T.U./(hr) (sq ft) (°F)}$$

for chloform and air and

$$h_o = 159 \text{ B.T.U./(hr) (sq ft) (°F)}$$

for the steam and air calculation, since a constant value of $h_c = 1{,}360$ was used for steam.

Evaluation of $U\Delta t$

The values of $U\Delta t$ at each point were calculated by substituting in equation (1) the previously determined variables, and solving for t_c by trial and error.

e.g. Point (2). *Chloroform and Air*

$$\frac{1}{h_o} = \frac{1}{h_a} + \frac{1}{h_c}$$

$$= \frac{1}{179} + \frac{1}{311}$$

$$h_o = 114 \text{ B.T.U./(hr) (sq ft) (°F)}$$

For $t_c = 87{\cdot}3$°F equation (1) becomes,

$$4{\cdot}5\,(115{\cdot}0 - 87{\cdot}3) + \frac{0{\cdot}448}{0{\cdot}523} \times 119{\cdot}4 \times 108{\cdot}5\,(0{\cdot}600 - 0{\cdot}330)$$

$$= 114\,(87{\cdot}3 - 59{\cdot}7) = U\,(115{\cdot}0 - 59{\cdot}7)$$

$$3121 = 3146 = 55{\cdot}3\,U$$

Average $U\Delta t = 3130$ B.T.U./(hr) (sq ft)

$U = 56{\cdot}6$ B.T.U./(hr) (sq ft) (°F)

and the hypothetical coefficient is

$$h_t = \frac{3130}{(115 - 87{\cdot}3)}$$

$$= 113 \text{ B.T.U./(hr) (sq ft) (°F)}$$

In the same way values of $U\Delta t$, U and h_t have been calculated for the other points. These final values are listed in Table 7 together with the values of q and h_o.

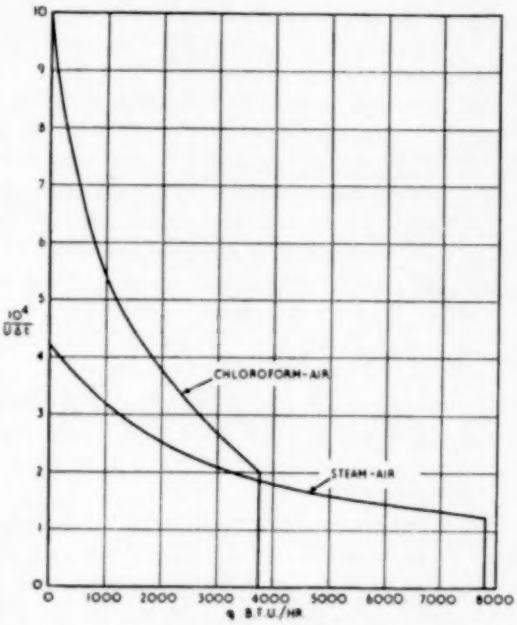

Fig. 2.

Table 7

System	*Point*	t_c °F	p_{gf}	K	h_o	$U\Delta t$	U	h_t	$\frac{10^4}{U\Delta t}$	q
Chloroform and air	(1)	88·3	0·483	1·15	179	5030	84·0	158	1·99	3781
	(2)	87·3	0·523	0·86	114	3130	56·6	113	3·19	2509
	(3)	81·7	0·577	0·683	107	2400	47·3	84·8	4·17	1658
	(4)	76·7	0·621	0·565	103	1830	39·8	64·7	5·46	996
	(5)	72·8	0·660	0·482	101	1420	34·4	52·2	7·04	499
	(6)	68·7	0·704	0·393	98	1000	28·2	39·5	10·0	0
Steam and air	(1)	121·4	0·737	1·59	159	8120	82·9	173	1·23	7795
	(2)	108·2	0·791	1·37	159	6260	68·7	121	1·58	5093
	(3)	97·0	0·842	1·20	159	4620	56·2	87·2	2·16	2851
	(4)	87·8	0·877	1·07	159	3310	45·3	63·4	3·02	1205
	(5)	84·0	0·891	1·02	159	2770	40·5	54·3	3·61	550
	(6)	81·0	0·906	0·98	159	2340	36·9	47·9	4·27	0

From a plot of $1/U\Delta t$ versus q, as in Fig. 2, equation (2) is graphically integrated to give the surface area required. The area obtained for the chloroform air system is 1·68 sq ft, which is equivalent to a condenser tube length of 5·94 ft. For the steam and air system, the area is 1·63 sq. ft., or 5·76 ft tube length.

The good agreement between the calculated areas and the expected area of 1·70 sq ft is apparent. It suggests that any further modification, such as that of SMITH is unnecessary, for the calculated area for the chloroform and air run agrees to within 2% of the expected and the calculated area for the steam and air run agrees to within 5%. Furthermore the modification of SMITH would lower the calculated area which would increase the deviation between calculated and expected areas. For these reasons the SMITH modification was not applied, nor was any other allowance made in the calculations for the cooling of the condensate.

The average condensate temperature, t_a, at the bottom of the condenser, obtained by taking the arithmetic mean of the wall temperature, t_m, and the condensate surface temperature, t_c, is calculate as 71·5°F for the chloroform and air system and 80·3°F for the steam and air system. These temperatures are lower than the expected average condensate temperatures of 86·0°F (30·0°C) and 94·1°F (34·5°C) for the respective chloroform and water condensate. This is perhaps due to reheating of the condensate by the gas-vapour mixture before it can be separated from the mixture in the experimental apparatus.

Colburn Approximate Method

The approximate method of COLBURN [3] outlined previously was also applied to both systems. The results of the calculations for this method are given in Table 8. For the value of h_c used here the effect of $^m/_{h_o}$ was quite considerable and in this case the accuracy of the method depends in part on the exact evaluation of the slope of the enthalpy versus temperature line. Actually the most difficult part of this calculation is the determination of m. The value of m in Table 8 was found as follows :

A plot of log p_v versus $\frac{1}{T}$ was made, as suggested by the Clausius-Clapeyron equation, over the temperature range involved in each case, i.e. from inlet to outlet t_g. From the resulting straight line $\frac{dp_v}{dt}$ was found. The value of $\frac{dH}{dp_v}$ is also known from the humidity-vapour pressure equation and hence by application of the function of a function rule $\frac{dH}{dt}$ results. Since m is evaluated at t_g, as suggested by COLBURN, m becomes $\frac{di}{dt}$.

Differentiation of equation (11)

$$i = \lambda_{32}\, H + c_s\,(t - 32) \qquad (11)$$

with respect to t. remembering that

$$c_s = c_{(air)} + c_{(vapour)} \times H \qquad (12)$$

and substitution of $\frac{dH}{dt}$ gives an equation for the value of $\frac{di}{dt}$ between the temperature limits chosen.

This method for evaluating the slope of the enthalpy line was found to be much simpler to

Table 8

	Chloroform and air		*Steam and air*	
	Top	*Bottom*	*Top*	*Bottom*
Vapour temp., t_g °F	120·2	94·0	168·3	129·9
Water temp., t_w °F	60·3	58·5	70·3	66·4
Vapour pressure, p_v atm	0·664	0·382	0·391	0·151
Enthalpy, i_g B.T.U./lb	1070	333	485	147
i_w*	105	101	26·6	23·5
Δi	965	232	458	123
m at t_g	29·5	5·70	7·93	1·96
h_g	5·37	3·02	8·13	5·74
c_s	1·38	0·60	0·42	0·29
h_o	179	98	159	159
(U_s/c_s)	2·37	3·89	9·85	15·9
Total B.T.U./hr	3781		7795	
(U_s/c_s) arith. average	3·13		12·9	
$(\Delta i)_{l.m.}$	515		255	
Calculated area sq ft	2·35		2·40	
Equivalent tube length ft	8·3		8·5	

VOL. 2 1953

use than standard mathematical methods, such as the Differentiated Gregory-Newton method and the Legrange Interpolation Method. As long as the temperature range involved is relatively small, so that the variation in latent heat of vapourisation is small, then the method is quite applicable.

Using this method the following equation was obtained :

$$\frac{di}{dt} = \frac{K' p_v M_v}{(1-p_v)^2 T^2 M_g} \left\{ \lambda_{32} + c_{(\text{vapour})} \times (t - 32) \right\} + c_s$$

where for chloroform and air $K' = 3030$

and for steam and air $K' = 3990$

The final value of the area required as shown in Table 8 gives areas for both calculations approximately 40% greater than is needed, which is reasonable considering firstly the assumptions on which the method is based and secondly the fact that an oversize area is obtained. For the cases studied the method is certainly conservative from the point of view of capacity.

Conclusion

The design procedure put forward by COLBURN and HOUGEN applied to known conditions has been found to give an area which is in good agreement with the expected area for the systems chloroform and air, and steam and air. The modification of this method proposed by SMITH has been found unnecessary.

The approximate method of COLBURN applied to the same conditions has been shown to give an area which is conservative from the point of view of capacity.

Acknowledgment

It is with pleasure that acknowledgment is made to Professor J. P. BAXTER for his assistance in this work.

Notation

A = area, sq ft
c = specific heat at constant pressure B.T.U./(lb) (°F)
c_s = humid heat B.T.U./(lb) (°F)
d = diameter of tube, ft
d_e = equivalent diameter, ft
D = diffusion coefficient, ft²/hr
dA = element of surface area
dq = increment of total heat transferred per unit time
g_L = acceleration due to gravity $4{\cdot}18 \times 10^8$ ft/(hr)²
G = mass velocity (lb/(hr) (sq ft)
h = film coefficient of heat transfer, B.T.U./(hr) (sq ft) (°F)
- h_a = combined water, metal wall and scale conductances
- h_c = condensate
- h_d = dirt or scale
- h_m = metal wall
- h_o = combined conductances other than the gas film
- h_s = gas film
- h_t = $dq/(tg - tc)\, dA$
- h_w = water film

H = humidity of mixture, lb/lb dry gas
i = enthalpy of saturated gas-vapour mixture, B.T.U./lb of dry gas
i_g = enthalpy of saturated gas-vapour mixture at t_g B.T.U./lb of dry gas
i_w^* = enthalpy of saturated gas-vapour mixture at the temperature of the cooling water B.T.U./lb dry gas
$(\Delta i)_{lm}$ = logarithmic mean of i_g and i_w^*
j = heat transfer or mass transfer factor
k = thermal conductivity, B.T.U./(hr) (sq ft) (°F/ft)
K = molar mass transfer coefficient, lb moles/(hr) (sq ft) (atm)
L = length, ft
m = slope of curve of i_w^* versus t
M = molecular weight
- M_a = air
- M_m = average gas-vapour
- M_v = condensable vapour
- M_g = inert gas

p = partial pressure, atm
- p_c = vapour pressure at t_c
- p_g = non-condensable gas partial pressure in the main body
- p_g' = that adjacent to condensate surface
- p_{gf} = logarithmic mean of p_g and p_g'
- p_v = vapour pressure

q = heat transferred, B.T.U./hr
T = absolute temperature, °R
t = temperature, °F
- t_a = average condensate temperature
- t_c = condensate surface temperature
- t_g = gas-vapour mixture temperature
- t_m = wall temperature
- t_w = water temperature
- Δt = overall temperature drop

U = over-all coefficient of heat transfer, B.T.U./(hr) (sq ft) (°F)
U_s/c_s = total gas-film heat transfer coefficient per unit enthalpy difference, B.T.U./(hr) (sq ft) (B.T.U./lb)

Γ = mass rate of flow, lb/(hr) (ft of wetted perimeter)

λ = latent heat of vapourisation, B.T.U./lb

μ = viscosity, lb/(hr) (ft)

ρ = density, lb/cu. ft.

$\mathrm{Pr} = \frac{c\,\mu}{k}$, Prandtl number

$\mathrm{Sc} = \frac{\mu}{\rho\,D}$, Schmidt number

$N_{Re} = \frac{D\,G}{\mu}$, Reynolds number

REFERENCES

[1] BROMLEY, L. A. and WILKE, C. R.; Ind. Eng. Chem. 1951 **43** 1641-8. [2] CHILTON, T. H. and COLBURN, A. P.; Ind. Eng. Chem. 1934 **26** 1183-7. [3] COLBURN, A. P. and Inst. Mech. Engrs. (London) Proc. 1951 **164** 448-58. [4] COLBURN, A. P. and HOUGEN, O. A.; Ind. Eng. Chem. 1934 **26** 1178-82. [5] PERRY, J. H.; Chemical Engineers' Handbook, 3rd Ed., p. 538, New York, McGraw-Hill Book Co. 1950. [6] PERRY, J. H.; *Ibid.* p. 476. [7] PERRY, J. H.; *Ibid.* p. 470. [8] SHERWOOD, T. K.; Absorption and Extraction, 1st Ed., p. 21, New York, McGraw Hill Book Co. 1937. [9] L. SILVER ; Inst. Chem. Engrs. (London) Trans. 1947 **25** 30-42. [10] SMITH, J. C. ; Ind. Eng. Chem. **34** 1248-52 (1942).

VOL. 2 1953

Chemical Engineering Science, 1953, Vol. 2, pp. 139 to 143. Pergamon Press Ltd.

Sulphur compounds in mineral oils

W. C. VAN ZIJLL LANGHOUT and H. I. WATERMAN

Department of Chemical Engineering, The Technological University of Delft, Holland.

(*Received* 1 *April* 1953)

Summary—A graphical statistical method is developed for the study of sulphur compounds in mineral oils.

The corresponding graphs are based on the ultimate analysis and physical constants and functions such as refractive index (n), density (d) and specific refraction $\left(\frac{n^2-1}{n^2+2}\cdot\frac{1}{d}\right)$.

A statistical graphical representation of the free enthalpy of formation of n-thiols, n-alkenes and H_2S, n-alkanes and sulphur is given.

Résumé—L'auteur propose une methode graphique et statistique pour la recherche des combinaisons sulfurées, présentes dans les huiles minérales. Les figures correspondantes sont basées sur l'analyse élémentaire et sur des constantes ou fonctions physiques comme n, d et $\frac{n^2-1}{n^2+2}\cdot\frac{1}{d}$.

L'auteur propose également une réprésentation graphique et statistique pour le potentiel thermodynamique moléculaire de formation des n-thiols, alkènes et H_2S, n-alkanes et soufre.

INTRODUCTION

To arrive at a better understanding of the composition of mineral oils the study of the sulphur compounds occurring in practically all these oils is of importance.

A preliminary investigation is made into the physical and chemical properties of sulphur compounds and of their mixtures either in the presence or in the absence of hydrocarbons.

A new method is proposed for improving our knowledge of sulphur compounds occurring in mineral oils and a thermodynamic study is made concerning possible conversions of sulphur compounds.

SECTION 1

About a year ago D. W. VAN KREVELEN [1] applied a new method in coal research by using graphs, based on the ultimate analysis of coal.

Such graphs can be also applied to mineral oils.

The majority of the mineral oils contain considerable quantities of sulphur compounds besides hydrocarbons. Compounds containing other elements such as oxygen and nitrogen in addition to carbon and hydrogen are generally only present in smaller quantities in mineral oils.

It is important to know which group of sulphur compounds is dominating or preponderant in the oil as one type may behave quite differently from the other. The type of sulphur compounds will have also a specific influence on the properties of the crude oil.

In Figs. 1 and 2, graphs are given for compounds which consist of C, H and S. These graphs can be applied to pure sulphur compounds or to mixtures of sulphur compounds. They enable the contruction of lines which represent the different groups of sulphur compounds.

Each defined sulphur compound is represented in the graph by a point, e.g. thiophene (C_4H_4S) in Fig. 1 by $H:C = 1{\cdot}00$ and $S:C = 0{\cdot}25$ and in Fig. 2 by $C:H = 1{\cdot}00$ and $S:H = 0{\cdot}25$.

In Fig. 1 hydrogen sulphide ($H:C = \infty$ and $S:C = \infty$) lies in the infinite.

Fig. 2 has the advantage that H_2S ($C:H = 0{\cdot}00$ and $S:H = 0{\cdot}50$) is represented by a point and that hydrogenation and dehydrogenation can be represented more clearly.

Two examples might illustrate how to use the graphs (c.f. Fig. 2):

From H_2S (C : H = 0·00, S : H = 0·50) and C_4H_{10} (C : H = 0·40 and S : H = 0·00) thiophene (C : H = 1·00 and S : H = 0·25) can be obtained resulting in a dehydrogenation. The equimolecular mixture of hydrogen sulphide and butane is represented by the point C : H = 0·33 and S : H = 0·083. From hydrogen sulphide H_2S (C : H = 0·00 and S : H = 0·50) and alkenes C_nH_{2n} (C : H = 0·50 and S : H = 0·00) thiols and thioethers can be formed, which are represented by points on line I.

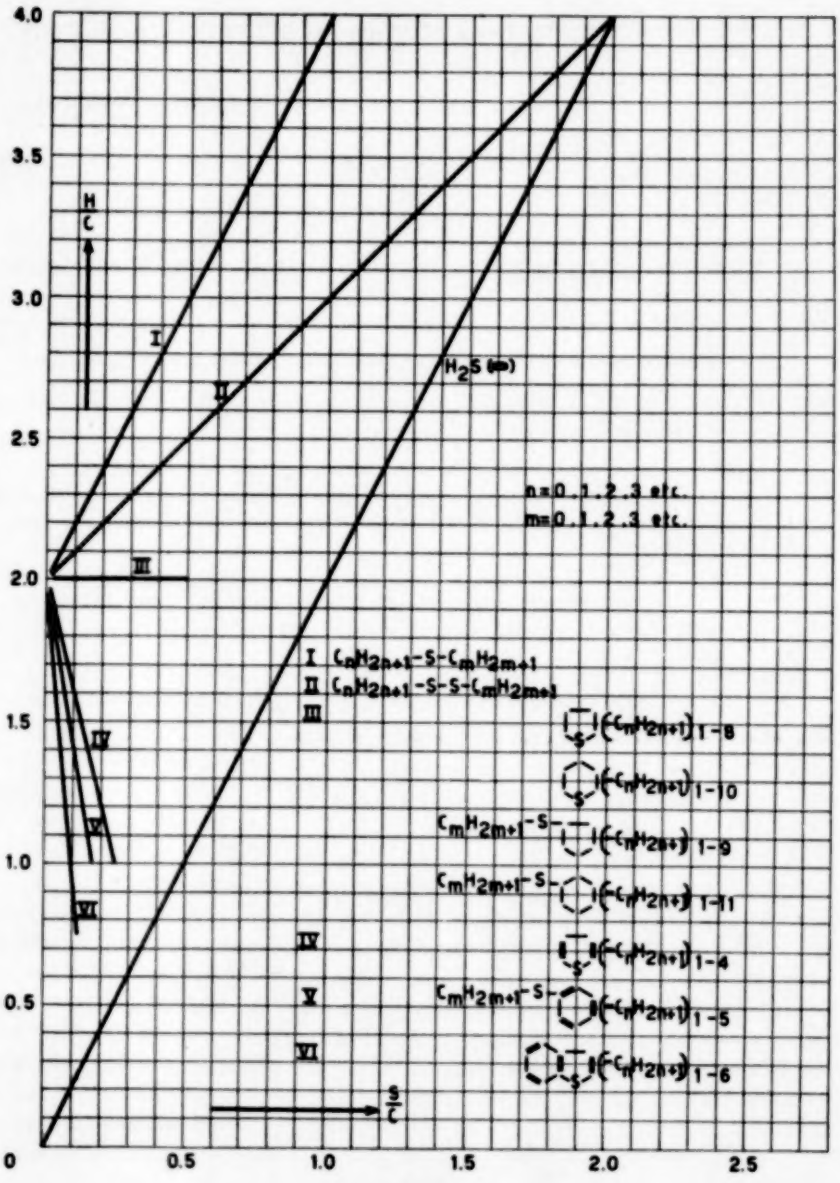

Fig. 1.

If a mixture of sulphur compounds has to be investigated and if this mixture is separated into fractions by physical means (adsorption, distillation) and if C —, H —, and S-determinations are done it is possible to get an impression of the composition of such a mixture. By determining the refractive index, density and molecular weight ($n - d - M$ method) even an accurate analysis should be possible. In such an investigation of crude oils the graphs discussed above could be of good help.

Suppose that a crude oil fraction containing sulphur compounds is exposed to an operation so that the composition is changed as a result of this. The investigation of the original fraction could be done as follows :

The fraction should be separated in two parts, i.e. hydrocarbons and a mixture of sulphur compounds. The hydrocarbons can then be investigated by means of the *n-d-M* method, the sulphur compounds by means of the graphs plus

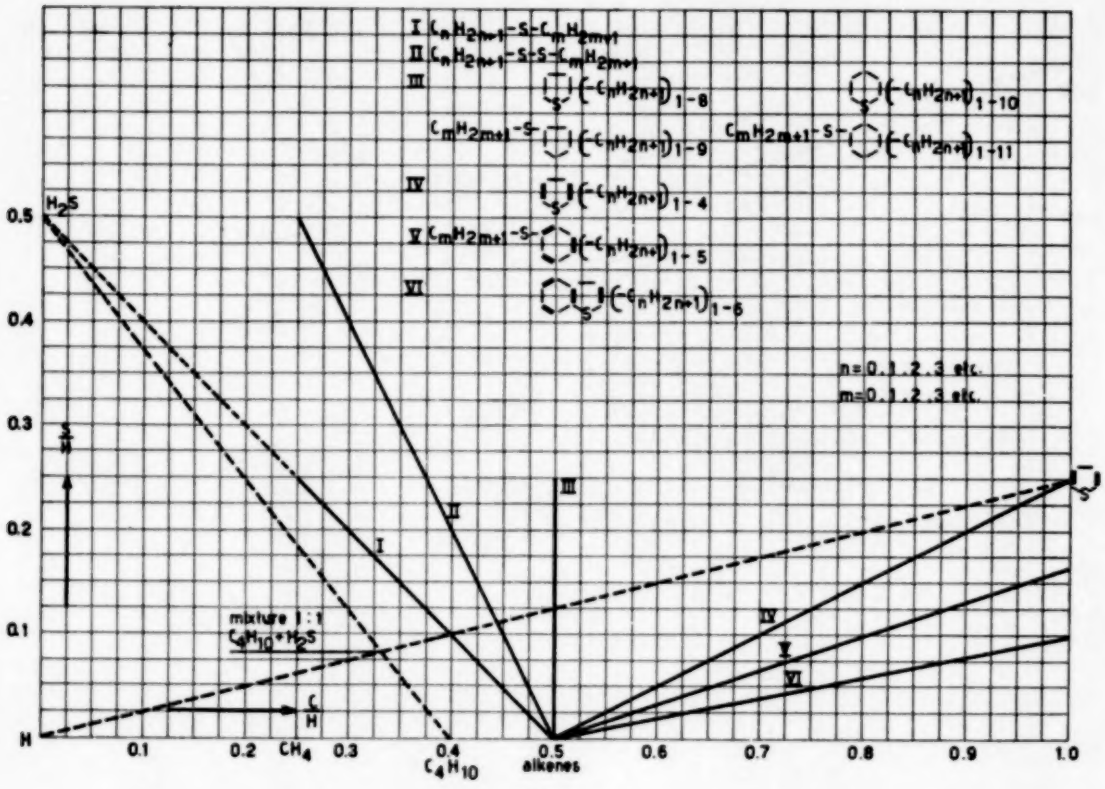

Fig. 2.

the determination of the refractive index, density, molecular weight and possibly other physical constants, the sulphur content and the ultimate analysis.

The operation with the original oil fraction is then carried out and the resulting product is investigated in an analogous way.

Thus it will be possible to obtain a certain knowledge of the behaviour of the hydrocarbons and of the sulphur compounds during the process. It might be possible that during the process sulphur compounds have been transformed into hydrocarbons and other sulphur compounds, whilst also hydrocarbons might react with sulphur compounds thus giving other hydrocarbons and sulphur compounds.

The main difficulty is the complete separation of hydrocarbons from sulphur compounds. Those sulphur compounds containing a high percentage of carbon and of hydrogen resemble very closely physically and chemically the corresponding hydrocarbons. There are indications that, in certain cases, a complete separation of hydrocarbons and sulphur compounds seems possible.

As a secondary problem there remains in certain instances the presence of oxygen and nitrogen compounds.

In the processes of synthesis of sulphur compounds from hydrocarbons and hydrogen sulphide, or from hydrocarbons and sulphur, or from hydrocarbons and sulphur compounds, the mixtures formed will not have such a complicated composition. Therefore such a synthesis can be more easily studied.

As the physical constants of a large number of sulphur compounds are already available it is possible to prepare a graphical representation as shown in Fig. 3. In this graph the specific

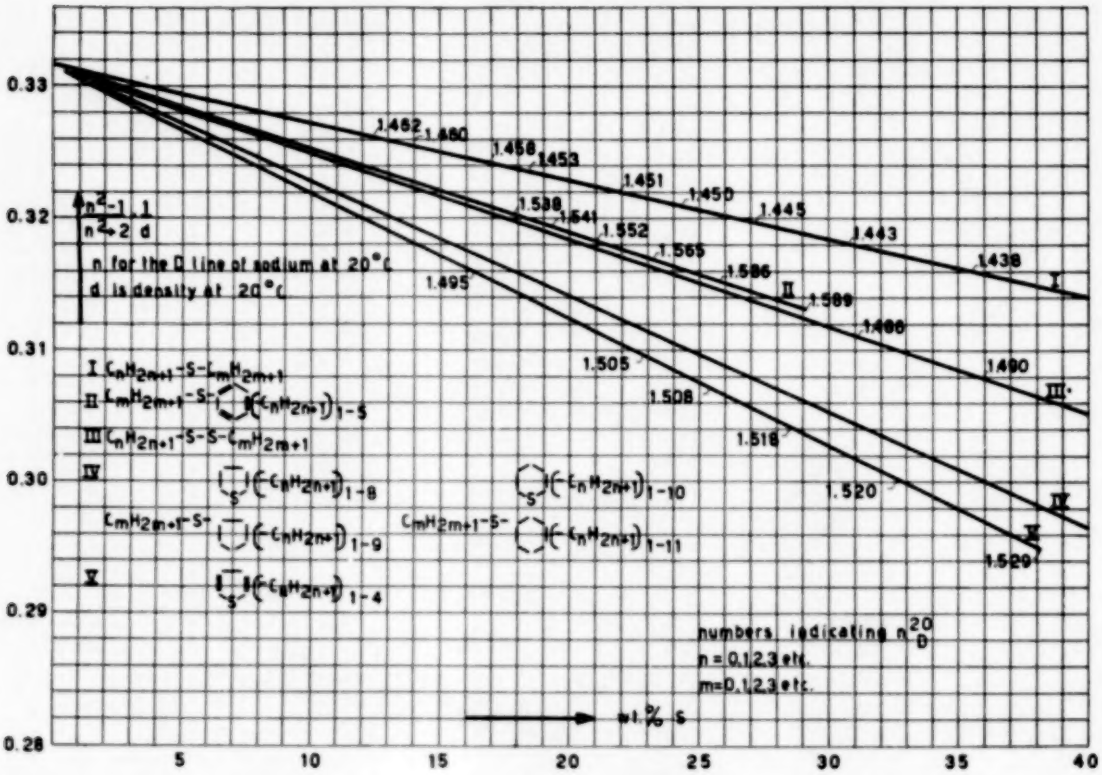

Fig. 3.

refraction $\frac{n^2-1}{n^2+2} \cdot \frac{1}{d}$ is plotted versus the percentage of weight of sulphur.

On the lines the values for n_D^{20} are indicated which enables an easy orientation. Fig. 3 is only of value if special types of compounds, e.g. strongly unsaturated aliphatic thiols have not to be taken into consideration.

The accuracy in the application cannot be compared with the *n-d-M* method for the analysis of hydrocarbon mixtures.

Nowadays an intensive study of sulphur compounds sponsored by the oil companies takes place all over the world. The graphs in question can be therefore improved gradually.

The present knowledge of the physical constants of many sulphur compounds already enables us to predict by inter-or extrapolation physical constants (n_D^{20}, d_4^{20}, boiling point) of sulphur compounds not yet investigated [2].

Section 2

For a more detailed study of the behaviour of sulphur compounds in mineral oils in the chemical and physical processes thermodynamical considerations cannot be omitted.

With the aid of the knowledge from the literature [3] it is possible to calculate the molecular free enthalpy of formation per C atom (ΔG_T° in kilocalories per mol. per C atom) from thiols, etc. (graphs in Fig. 4).

The molecular free enthalpy of formation is plotted versus the number of C atoms. The n-thiols have been compared with the n-alkenes-1 and hydrogen sulphide and with the n-alkanes and sulphur. The graphs are valid for the gaseous phase at one atmosphere.

For the temperatures 300°K, 500°K and 800°K, respectively, the curves are calculated and given in Fig. 4. From the place of the curves

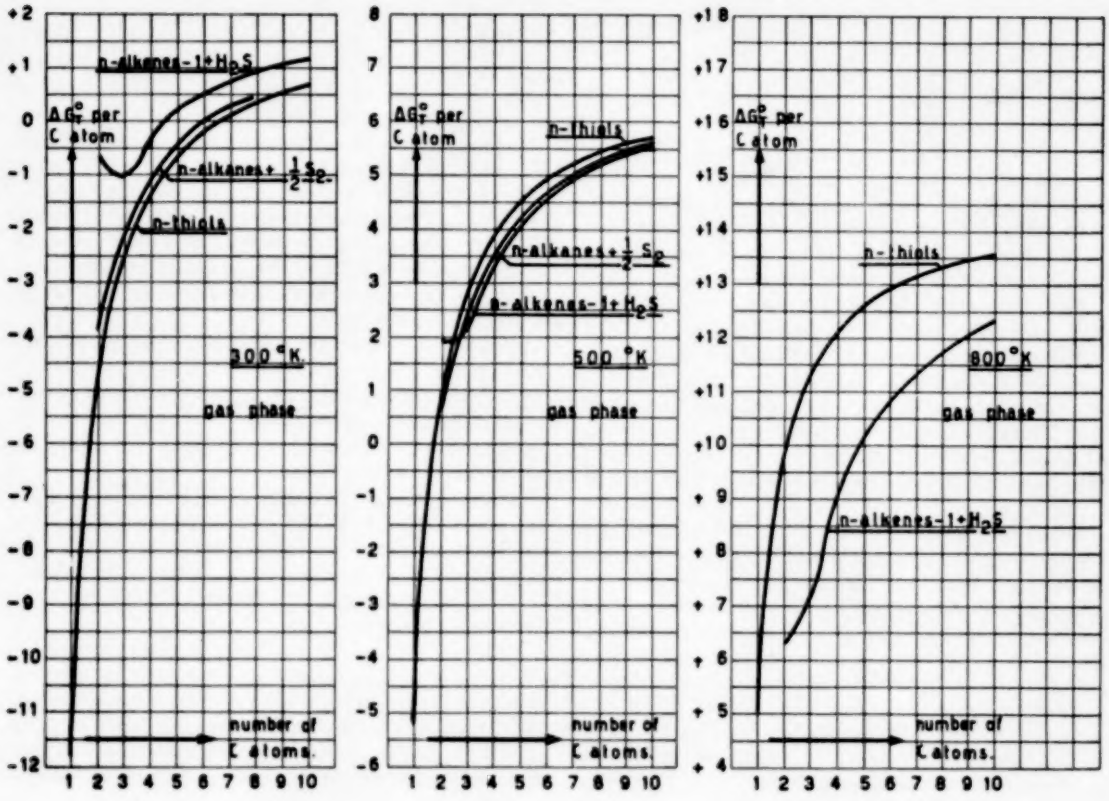

Fig. 4.

in the diagram the stability of the considered compounds can be derived.

At 300°K the normal thiols are stable compared with the corresponding n-alkenes-1 + hydrogen sulphide and stable compared with the n-alkanes + sulphur.

At 500°K the thiols are just metastable compared with the systems mentioned. If the rate of reaction would be high enough the normal thiols could decompose in n-alkenes-1 + hydrogen sulphide at 500°K and 1 atmosphere. Thus could be explained the formation of hydrogen sulphide in the final distillation of refined crude oil fractions which still contain sulphur compounds.

From the graphs it can also be concluded that alkanes can be transformed by dehydrogenation with sulphur into alkenes.

These graphs have not a quantitative value as their basis is not quite certain. In the near future it may, however, be expected that more thermodynamical data will be available, as recent literature shows thermodynamical properties even of higher sulphur compounds in the preparation of very pure sulphur compounds.

LITERATURE :

[1] VAN KREVELEN, D. W. ; Fuel **29**, 1950 269. [2] WHITE, P. T., BARNARD-SMITH, D. G., FIDLER, F. A. ; Ind. Eng. Chem. **44** 1952 1430. [3] VAN KREVELEN, D. W., CHERMIN, H. A. G. ; Chem. Eng. Sc. I 1951 66 ; I 1952 238.

Book review

Dr. Ing. Wilhelm Gumz: Vergasung fester Brennstoffe, Springer-Verlag, Berlin, Göttingen, Heidelberg, 1952. 102 pp. 4 illustrations. DM 9.60.

The author has typified the matter dealt with in his book by the sub-title, *Stoffbilanz und Gleichgewicht – Eine Darstellung praktischer Berechnungsverfahren.*

The author restricts himself mainly to a discussion of the various methods developed for calculating the equilibrium composition of gases that may be produced when solid fuels are converted with gasifying agents.

Moreover, these calculation methods are illustrated by examples in which even the formation of sulphur-containing compounds, such as H_2S, COS, CS_2 has been reckoned with. It is regrettable that no use is made in these examples of the heat balances that may be drawn up, although the drawing up of such balances in general is dealt with in a separate section.

It is owing to the omission of the heat balances, that the results of some of the calculation examples given differ considerably from those obtained in practice.

This applies for example to the first (and very simple) example of a process according to which pure carbon is gasified in counter-current with dry air at atmospheric pressure and the equilibrium composition of the gas is calculated at a temperature of 650°C (p. 70). However, in adiabatic systems the equilibrium temperature in the gasification of coke, carried out with dry air of room temperature, is easily twice as high.

This explains why in practice it is quite possible by means of cold dry air to produce a gas containing less than 1 per cent of CO_2, instead of the 9·89 per cent stated by the author.

Those who should feel inclined to adopt the calculation examples given here as a guide for carrying out equilibrium calculations, must be well aware that in order to obtain practically useful results, the character of the gasifying agent on the one hand and the height of the equilibrium temperature on the other hand may not be selected independently of each other, but that the relationship between these two factors must be calculated with the help of a heat balance.

As the author has prefaced his main subject by a rather extensive general introduction to the gasification theory, his book deserves more general interest than might be aroused by the sub-title. The introduction is certainly worth reading, although the critical reader will not be entirely satisfied by it.

For example, many will rightly have doubts as to the truth of the statement that in practice the Boudouard equilibrium and the water gas equilibrium should always be attained (p. 22), although it must be admitted that the value of the equilibrium calculation for the gas technician can be hardly overestimated.

In the chapter on the kinetics of the gasification reaction, the author emphasizes the great difference between the carbon temperature and the gas temperature that may occur during the gasification process, as well as the influence of the physical transport resistance on the rate of the gasification reaction.

However, the remark made in this connection to the effect that at temperatures of from 700-750°C the physical resistance should already far exceed the chemical resistance is certainly not acceptable. Generally speaking, this only holds for the reaction between carbon and oxygen but not for reactions between carbon and carbon dioxide or steam.

Although some more remarks of this kind might be made, this does not alter the fact that it is very desirable to possess a book in which the various methods for calculating the gas equilibria are collected and which contains an introduction in which an expert confronts the reader with the more fundamental problems connected with the gasifying process.

W. van Loon.

VOL. 2 1953